THE PENNSYLVANIA STATE UNIVERSITY
SCHREYER HONORS COLLEGE

COLLEGE OF AGRICULTURAL SCIENCES
ENVIRONMENTAL RESOURCE MANAGEMENT

Modeling Vernal Pool Basin Morphology above the Headwaters of the Appalachian Mountains

RITVIK PRABHU
FALL 2021

A thesis
submitted in partial fulfillment
of the requirements
for a baccalaureate degree
in Environmental Resource Management, Water Science
with honors in Environmental Resource Management

Reviewed and approved* by the following:

Jonathan M. Duncan
Assistant Professor of Hydrology
Thesis Supervisor

Robert Shannon
Associate Professor of Agricultural and Biological Engineering
Honors Adviser

* Electronic approvals are on file.

ABSTRACT

Vernal pools are seasonal, depressional wetlands that typically become inundated in the winter and spring and then dry up in the summer and fall. They offer a number of important ecosystem services including providing habitat for amphibian reproduction and other aquatic life, accumulating organic matter, and facilitating enhanced nutrient cycling. The US Environmental Protection Agency states that human activity has caused large percentages of recorded vernal pools to be impacted or destroyed by development and pollution. To properly regulate and protect vernal pools, reliable delineation methods are needed to identify vernal pool locations and characterize basin morphology. Although the term 'vernal pool' is used homogenously across the United States, vernal pools can differ by region in morphology and hydrologic regime. This variability makes it difficult to create generalized delineation methods. The Wetland Hydrology Analyst Toolbox (WHAT) is an approach developed for use in the Prairie Pothole Region that has proven effective in delineation. This thesis applied the WHAT to the Northern Ridges and Valleys region of the Appalachians to see whether eleven small forested vernal pools could be detected and accurately depicted. Optimal parameters of this toolbox were compared to other notable delineation methods—aerial imagery analysis represented by the National Wetlands Inventory (NWI) and object-based imagery analysis (OBIA) represented by a 2013 dataset of Pennsylvania wetlands—along with manual measurements and local knowledge to determine accuracy levels. The NWI method was found to be the most accurate, with the OBIA method less accurate, followed closely behind by the WHAT method. Although the least accurate, the WHAT has the potential to improve data quality by adjusting the parameter values or by revising the Python scripts to cater more to the region.

TABLE OF CONTENTS

LIST OF FIGURES

LIST OF TABLES

ACKNOWLEDGEMENTS

Thank you to my thesis supervisor Dr. Jonathan Duncan for introducing me to the world of research and for fostering a positive environment for creativity and the pursuit of science, the way it should be.

Thank you to Ph.D. student Taylor Blackman for all of his guidance in fieldwork, GIS skills, and the research process. Special thanks for providing without hesitation whatever maps, data, and images I needed. I have learned so much from you this year and thoroughly enjoyed the days spent out in the Ben Jacobs Trail saddle.

Thank you to Dr. Robert Shannon for being such a friendly, available, helpful honors adviser. You have made my experience at Penn State so much more enjoyable and manageable.

Thank you to the College of Ag. Sci. (CAS) and Undergrad. Education Office for providing summer research funding through the CAS Undergrad. Summer Research Grant.

Thank you to Jonathan Chester for the time-saving recommendation that I use the Wetland Hydrology Analyst Toolbox (written in Python 2 code) in ArcMap.

Thank you to the rest of the Duncan Lab Group for being so welcoming when I first joined and for opening my eyes to so many different avenues of hydrologic research.

Thank you to Matthew Bellia and Connor Price for assisting with fieldwork pool measurements. Thanks to Matthew for fixing the spool measurer after it jammed.

Thank you to all those whose research I used in this paper, especially Dr. Qiusheng Wu and Dr. Charles Lane for creating such an interesting toolbox, as well as all those like PASDA who provide open-source data and software.

Finally, thank you to my family and friends for all of their support. I have loved my time here at Penn State, and you are a large reason why.

Chapter 1

Thesis Statement

Vernal pools are seasonal, depressional wetlands that often fill with water in the winter and spring and experience drawdown in the summer and fall (EPA, 2021b). While the term ‘vernal pool’ is used homogenously across the United States, vernal pools can differ by region in morphology (e.g., shape, size, depth) and hydrologic regime (e.g., how quickly water tables rise in response to storm events, time of total drawdown in the growing season) (Machtinger, 2007). Vernal pools offer a range of ecosystem services, including the provision of habitat for amphibian reproduction and other aquatic life, the accumulation of large amounts of organic matter, and the facilitation of enhanced nutrient cycling, all largely a function of their hydroperiod (length of wetness) and morphology (Colburn, 2004).

Human activity, such as development and pollution, has decreased recorded vernal pool numbers by as much as ninety percent in some states (EPA, 2021b). Because of their classification as geographically isolated wetlands (GIWs), vernal pools are not protected under the Clean Water Act ever since the 2006 Supreme Court *Rapanos vs. United States* decision (Tiner, 2003; EPA, 2021a). Some states, including Pennsylvania, have protections for vernal pools, but are limited by the underrepresentation of pool numbers in wetland inventories (PennDOT, 2015; Lathrop et al., 2005).

Vernal pool inventories and delineations are time consuming to create from field surveys and made more difficult in the Appalachian portion of Pennsylvania, due to remote locations, rugged terrain, and dense vegetation. Aerial imagery analysis offers a remote option for delineation, but still requires a lot of time and labor. Technological advances in mapping and software have led to the application of automated methodologies in wetland identification. One such method is the Wetland Hydrology Analyst Toolbox (WHAT) developed by Wu & Lane (2017). This toolbox had marked success delineating GIWs in the Prairie Pothole Region of the United States, but it is unknown how it would perform with smaller depressions in hillier terrain.

The purpose of this thesis is to apply the prairie pothole delineation capabilities of the open-source WHAT to a select number of Northern Ridges and Valleys forested Appalachian vernal pools (FAVPs) and to compare the resultant morphology characteristics to those of more established delineation methods (field inventory, local knowledge imagery analysis, National Wetlands Inventory (aerial imagery analysis), and object-based imagery analysis).

Although the WHAT was developed for prairie potholes with an estimated median size of 1600 sq. meters, the nature of contour delineation as well as the ability to specify contour intervals creates a possibility for this toolbox to work on FAVPs that are often smaller than 400 sq. meters (Wu & Lane, 2017; Brown & Jung, 2005). An automated delineation process with reliable morphology metrics would have major significance for FVAP inventory and conservation efforts, especially given the lacking body of information about FVAP morphology (Blackman, 2019).

H_0: There will be no improvement in pool identification or morphology measurement accuracy when using the WHAT compared to more established delineation methods.

H_A: There will be improvement in pool identification or morphology measurement accuracy when using the WHAT compared to more established delineation methods.

Chapter 2

Background

2.1 Vernal Pool Definitions

The term ‘vernal pool’ first originated in the early 20th century, to describe small seasonal wetlands in the Western United States, but was eventually expanded nationwide. The general Environmental Protection Agency (EPA) description for a vernal pool is a seasonal, depressional wetland that tends to become inundated with water in the winter and spring and dry out in the summer and fall. Pools are largely found in Western United States grasslands or in glaciated regions of the Northeast and Midwest (Huertos, 2020; EPA, 2021b).

The broadness in definition leads to the inclusion of a variety of pool characteristics. For example, the EPA description continues further by saying vernal pools can range in size from puddles to lakes and can either be connected or isolated (EPA, 2021b).

Making matters more difficult is that vernal pools are only one kind of temporary wetland. Other prominent examples include playas—shallow, seasonal or semipermanent depressions found in the South-Central Plains—and prairie potholes—semipermanent larger depressions in the Upper Midwest region (Machtinger, 2007). As these descriptions demonstrate, it can be difficult to differentiate between temporary wetlands without a deeper understanding of their identities. Since there is no definitive consensus in the scientific community on the terminology for each of these wetlands, it is normal for one piece of literature to combine vernal pools with other temporary wetlands, while another views them as distinct (Tiner, 2003). Figure 2.1 displays one interpretation of categorizing vernal pools. The Cowardin 1979 classification system, employed by the EPA, views vernal pools, playas, and prairie potholes all as Non-tidal Marshes (EPA, 2016). This seems an oversimplification, given how variable the wetlands are.

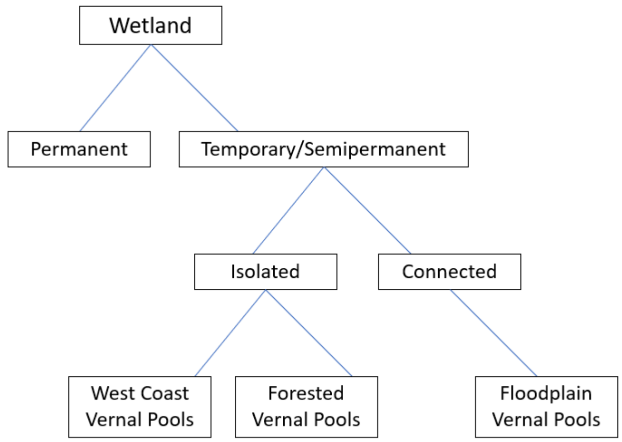

Figure 2.1 One interpretation of vernal pool categorization. Created in PowerPoint (Microsoft, 2021b)

Another attempt to group these wetlands together is by calling them geographically isolated wetlands (GIWs). As the name suggests, a GIW is a wetland that, while it may at times be hydrologically connected with nearby wetlands and bodies of water, exists physically surrounded by upland. While Leibowitz & Brooks (2008) found that geographic isolation is not a component of all Northeastern vernal pools, this term adequately represents West Coast vernal pools and forested vernal pools nationwide (Tiner, 2003). The forested Appalachian headwaters of the Northeast can therefore be considered GIWs.

2.2 Appalachian Headwaters Vernal Pools

This thesis focuses on vernal pools located in the Northern Ridges and Valleys region of the Appalachian headwaters, which have specific characteristics of their own. Henceforth, the term ‘forested Appalachian vernal pool (FAVP)’ will refer to solely these pools, unless specified otherwise.

Leibowitz & Brooks (2008) established three distinguishing features of Northeastern vernal pools, including FAVPs. The first is existence within a previously glaciated forest region. The Northern Ridges and Valleys can be considered peri-glaciated, since the glaciers near central Pennsylvania exerted a topographic and climatic influence beyond their boundaries (Marsh, 1999). The last two features are a constantly changing hydrology and seasonal inundation. Characteristic of a vernal pool, FAVPs experience seasonal fluctuations with pool expansion in the winter and spring and drawdown in the summer and fall. The magnitude of the seasonal shift depends on annual precipitation levels and average annual temperatures (Leibowitz & Brooks, 2008). This creates the degree of randomness that makes characterizing vernal pools so difficult.

Despite often being grouped together, FAVPs are very different morphologically and hydrologically from other GIWs like prairie potholes or California vernal pools. FAVPs on the whole are much smaller in size and have distinctive water budgets (Machtinger, 2007; Blackman, 2019; Brown & Jung, 2005). California vernal pools and prairie potholes rely on direct precipitation and runoff inputs for a large part of their inflow, while FAVPs’ existence in hilly topography can lead them to have significant groundwater and subsurface flow inputs in addition to whatever direct runoff and precipitation they receive. Although there is often a groundwater influence for every wetland, it is more closely tied to a FAVP’s water budget expression. At times, FAVPs can form solely because of an elevated groundwater table and therefore do not require a confining bottom layer (Figure 2.2) (Tiner, 2003; Leibowitz & Brooks, 2008).

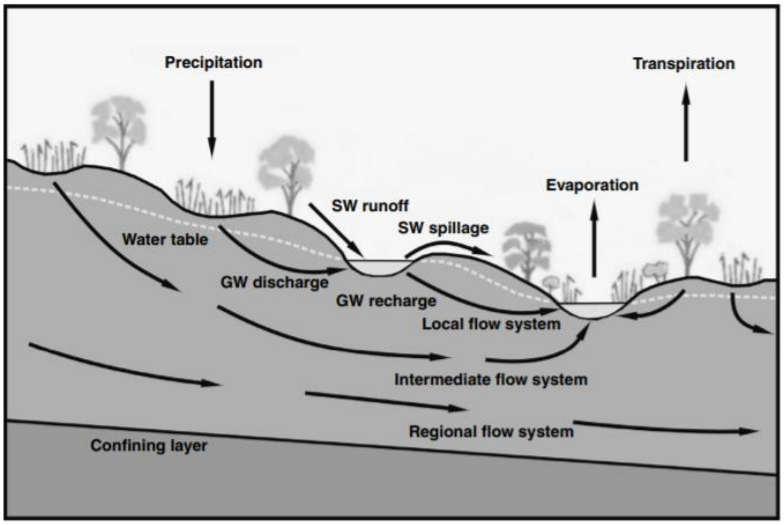

Figure 2.2 Northeastern Vernal Pool water budget from (Leibowitz & Brooks, 2008)

One more major difference is the increased difficulty to identify and delineate FAVPs versus prairie potholes and California vernal pools. FAVPs' small size and their surrounding landscapes' abrupt transitions in bedrock type, soil properties, forest cover, and how surface hydrology is expressed present far more mapping challenges than those of their larger, more-open contemporaries (see Figure 2.3) (Jensen et al., 2019). Stolt and Baker (1995) found that the total number of GIWs located in the Southern Blue Ridge of Virginia may be significantly more than those accounted for in the National Wetlands Inventory. Perhaps because of these reasons, there exists far less scientific literature for FAVPs than for prairie potholes or Western vernal pools and the true number of FAVPs is largely unknown (Blackman, 2019).

Figure 2.3 Larger, more-open Prairie Potholes (top left) and California Vernal Pools (top right), from (Machtinger, 2007), compared to a Forested Appalachian Vernal Pool (bottom)

2.3 Vernal Pool Ecosystem Services

Despite the limited research in many areas concerning FAVPs, it is well established that FAVPs provide a host of ecosystem services. These wetlands act as intermediary collection points for surface and subsurface drainage, temporarily storing water before releasing it downgradient to tributaries, waterways, and drinking water supplies. This water storage system helps to lower peak flow rates and raise times of concentration, thereby decreasing erosion and flooding. FAVPs also contribute to groundwater recharge and can have groundwater connections ranging from the local to the regional scale. Soluble materials, like organic matter and nutrients, enter the pools in the form of plant and animal detritus and are transported by these groundwater channels to other waterways. Groundwater that leaks out from the perimeter of the pools provides a water source to plants and encourages evapotranspiration which helps fuel the hydrologic cycle (Leibowitz & Brooks, 2008).

The fluctuating level of inundation and saturation creates the perfect conditions for alternating biogeochemical processes. For example, in the summer and fall, aerobic nitrification converts collected ammonium to nitrates, which stimulates plant and algae growth. In the winter and spring, anaerobic denitrification dominates, helping to remove excess nitrates and reduce potential eutrophication. Similarly, phosphorous-adsorbed sediment can settle out in the temporary storage basins, rather than washing into downgradient waterways (Fisher and Acreman, 2004).

Perhaps the most important service FAVPs provide is as a habitat for a variety of species. Because FAVPs have no permanent surface water connection to other waterways, they are devoid of fish species. This relieves a major source of predatory pressure on the amphibian and invertebrate species that breed within the pools. FAVPs also provide habitat for many plants, including the endangered Northeastern Bulrush (*Scirpus ancistrochaetus*), as well as act as drinking and food sources for numerous species of birds and mammals. The vernal pools within Pennsylvania, both FAVPs and otherwise, support six amphibian species and two crustacean species that are considered obligate species, meaning they rely solely on vernal pools to breed. This includes well-known species like the Spotted Salamander (*Ambystoma maculatam)* and threatened species like the Eastern Spadefoot toad (Scaphiopus holbrooki) (see Table 2.1) (WPC, 2018). In fact, within the Mid-Atlantic region, 26% of all state-designated threatened and extinct amphibians rely on vernal pools for habitat (Brown & Jung, 2005).

Table 2.1. Examples of amphibians that use Pennsylvanian vernal pools for reproduction from (Julian, 2018)

Vernal Pool Amphibians:
Amphibians in The Barrens that need vernal pools

	Common name (Scientific name)	*NatureServe* Conservation Rank
	Eastern spadefoot toad *(Scaphiopus holbrookii)*	S2 Imperiled / S3 Vulnerable
	Jefferson salamander *(Ambystoma jeffersonianum)*	S3 Vulnerable
	Marbled salamander *(Ambystoma opacum)*	S3 Vulnerable
	Spotted salamander *(Ambystoma maculatum)*	S5 Secure
	Wood frog *(Lithobates sylvaticus)*	S5 Secure

S5 Secure = Common, widespread, and abundant in the state
S2 Imperiled = Rarity due to very restricted range, very few populations (often 20 or fewer), steep declines, or other factors making it very vulnerable to extirpation from the state
S3 Vulnerable = Vulnerable due to a restricted range, relatively few populations (often 80 or fewer), recent and widespread declines, or other factors making it vulnerable to extirpation

The ephemeral nature of vernal pools produces a challenging environment that aquatic life handles by using adaptive advantages. For example, amphibians are able to develop in water and then live as adults on land, while fairy shrimp lay dormant eggs in the soil until the next period of inundation. The expectation, however, is that the pool will have surface water for a certain portion of the year. Even while on land, amphibians live in close proximity to their pools and eighty-five percent of these amphibian species will breed in the same pool that they were born in (PNHP, 2019). Therefore, if a pool dries out or is damaged one year, a local extinction can occur. Occasional local extinctions are natural and when the pool fills up the next year, repopulation can occur from nearby pools. For this system to work, however, enough pools need to exist in the area and transportation corridors need to be present, such as land for amphibians and spillways for fully aquatic species (Leibowitz & Brooks, 2008).

The number of vernal pools has been declining nationwide. Deliberate destruction for development and agricultural space as well as indirect destruction by logging operations, groundwater drawdown, and water quality pollution can lead to habitat fragmentation and impact nearby pools (Brown & Jung, 2005). Reductions in California vernal pools have been found to be as high as ninety percent (EPA, 2021b). Because of how under-documented FAVPs are, there is no way to know how many have been impacted. It is reasonable to estimate that the minimum is a similar value to the total documented wetland loss in Pennsylvania—fifty percent (PNHP, 2019).

Efforts to preserve FAVPs are hindered by regulatory issues. The Clean Water Act 1972 amendment established federal oversight for all navigable ‘waters of the United States’ (WOTUS). The exact interpretation of WOTUS was left open-ended and resulted in several court cases. The most significant of these cases was the 2006 Supreme Court *Rapanos vs. United States* decision. It found that only wetlands with a continuous surface connection could be considered WOTUS. A concurring decision from that case included wetlands that had some form of ‘significant nexus’ with the permanent waterways. Although administrations have changed the definition every few years, FAVPs remain largely unprotected (EPA, 2021a).

Conservationists have therefore had to fall back on two options. The first is gaining protection under the Endangered Species Act of 1973 by providing evidence that the pool(s) in question provide habitat to a species on the Endangered Species list (PNHP, 2019). The second is implementing increased protections under state law. In Pennsylvania, the Dams Safety and Encroachment Act (DSEA) gives discretion to the Pennsylvania Department of Environmental Protection to decide whether to issue permits for wetland development and to what degree of impact that development will be. Only wetlands greater than 0.05 acres (~200 sq. meters) are required to be replaced, restored, or enhanced upon disturbance, unless they are considered of 'exceptional value' (CoP, 2021; BWEW, 2021). The United States Geological Survey Northeast Amphibian Research and Monitoring Initiative conducted a survey of 134 Mid-Atlantic vernal pools and found that seventy eight percent of them were smaller than 400 sq. meters, which indicates that a significant portion of FAVPs do not apply for that protection under DSEA (Brown & Jung, 2005). Even with legal protection, conservation efforts are limited without a proper inventory of FAVPs. Properly delineating FAVPs is crucial to both preserving them and understanding the total benefit they bring to local and regional ecosystems.

2.4 Methods of Delineation

To accurately identify and delineate FAVPs, several different methods have been developed. Each has its own benefits and limitations and often can have successes in one area and difficulties in another. Research is ongoing to develop more effective, efficient procedures.

2.4.1 Field Inventory and Manual Measurement

Considered to be the most accurate, this method employs a 'boots on the ground' approach, by having individuals perform walkthroughs of an area to manually find the locations and measurements of the pools there. The accuracy of the data relies on proper understanding by the data collectors of how to recognize vernal pools and how to identify the extent of a pool boundary. FAVPs are often in highly vegetated, rocky topography, which is not conducive to manual delineation, so it is recommended inventories be performed in early spring while pool levels are high and before leaf-out has occurred. This method demands a large amount of time and labor and so is only practical for small, localized areas or to get reference values to compare experimental values against. This process can be made more efficient by using aerial imagery or Geographic Information System (GIS) mapping to determine areas with a suspected high density of pools, thus helping to narrow areas of interest (AOIs). If done properly, this method will yield no commission errors (including a pool when no pool exists) and very few to no omission errors (not including a pool when a pool exists). The Pennsylvania Vernal Pool Registry was created through the Pennsylvania Natural Heritage Program as a way for citizen scientists to begin identifying FAVPs and other vernal pools throughout the state (PNHP, 2019). Although the data is likely not as systematically or accurately collected as that from a professional inventory, it represents an example of manual inventories and measurements in action.

2.4.2 Aerial Imagery and LiDAR Hillshade Analysis

This method involves the creation of maps that emphasize changes in the topography, making the identification of water-filled depressions easier. Aerial imagery is photographs collected by a low-flying drone, plane, or helicopter. The photographs are ideally taken on clear days in leaf-off seasons (late fall to early spring) (see Figure 2.4).

Figure 2.4 Leaf-off 2018-2020 aerial display imagery from Pennsylvania Spatial Data Access Imagery Navigator (PASDA, 2018-2020). Scale is 1:4,513

LiDAR (Light Detection and Ranging) is acquired from a plane equipped with a laser that emits pulses of infrared light towards the ground to accurately measure distance. When the light reflects off the surface it moves back towards the plane, where it is picked up by a scanner (see Figure 2.5). The amount of time it takes for the light to return determines the elevation of the reflecting point. The latitude and longitude of the point is calculated by a Global Positioning System (GPS) receiver, with the angle of reflection and movement of the plane accounted for. The return times of surrounding points helps to determine whether the point in question is the bare ground or an elevated surface like a tree or building. The intensity of the reflected light can also be used to determine the material of the reflecting surface. This can be used to determine land use at that point or predict what kind of object it is (NOAA, 2021; GISGeography, 2021). LiDAR data are also ideally recorded in leaf-off seasons for wetland mapping.

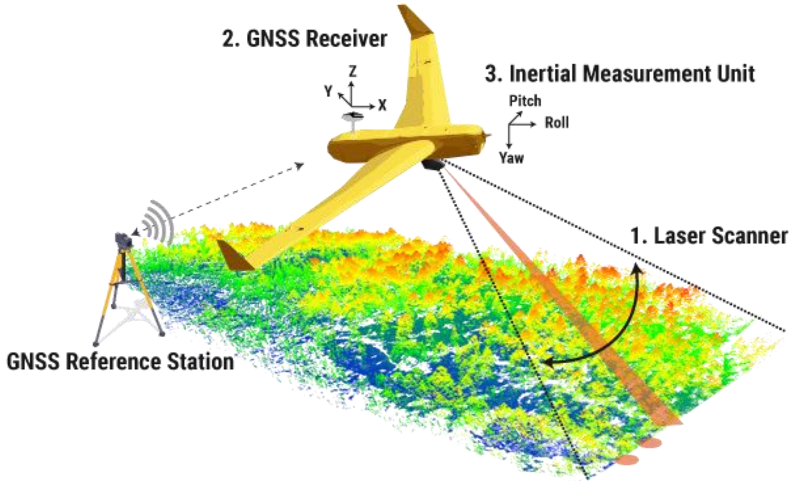

Figure 2.5 Diagram of the collection and calculation of Light Detection and Ranging point cloud data from (YellowScan, 2020)

The result of this process is the collection of thousands of points that contain at least latitude, longitude, and elevation values. These points make up what is called a data point cloud, which is often stored in .las format. This LiDAR point cloud data can then be converted to raster format through GIS software (see Appendix D). The conversion occurs by taking a group of points and interpolating a single elevation value from them. This creates a raster grid, also known as a Digital Elevation Model (DEM), with far less noise that depicts the topography of the AOI in a 2D format (see Figure 2.6).

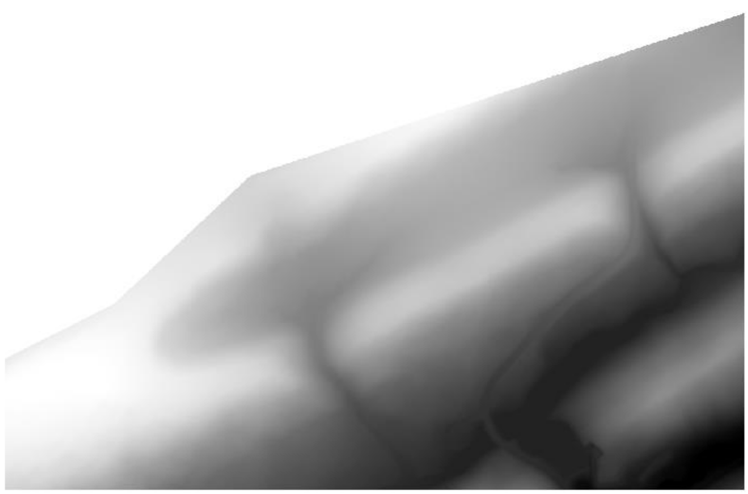

Figure 2.6 United States Geological Survey 2017 LiDAR Digital Elevation Model from Pennsylvania Spatial Data Access database (USGS, 2017). Viewed in ArcGIS Pro (Esri, 2021a)

To create an even clearer image of the topographic surface, the DEM can be converted to a hillshade format, where shading is incorporated to create a 3D-looking surface. An ideal hillshade for delineation is created by using a geoprocessing tool to fill all the depressions in a DEM (see Appendix F) and then using an arithmetic tool to subtract the original DEM's elevation values from this new DEM's elevation values. From this hillshade, depressions are far more evident since the surrounding area is all flat (see Figure 2.7).

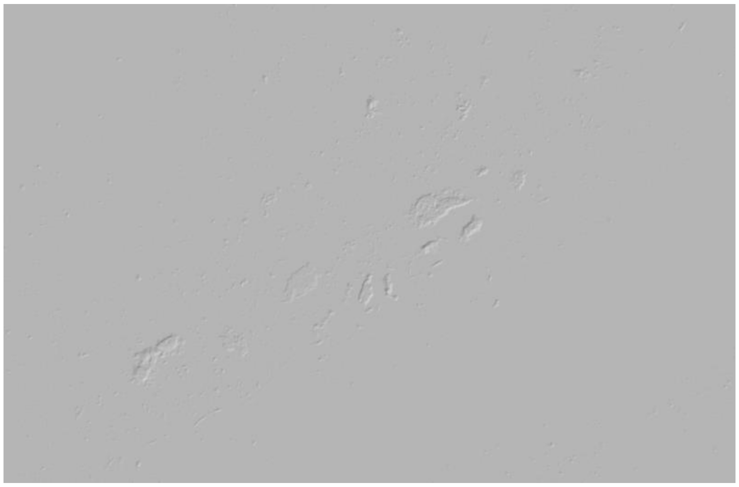

Figure 2.7 Hillshade DEM clearly showing surface depressions. Created in ArcGIS Pro (Esri, 2021a). Original DEM from (USGS, 2017)

Aerial imagery can very clearly show FAVPs when they are large, filled with water, and not covered by vegetation or canopy cover. Should conditions at the time of image acquisition not be ideal (e.g., due to clouds, reflections, shadows), the hillshade DEM can offer a way to visualize ground surface regardless of vegetative cover and to notice relative lows and depressions in an area. Aerial and hillshade imagery are often manually viewed together and the pools are delineated and then digitized if the delineation was done on paper (less likely nowadays).

The National Wetlands Inventory (NWI) is the most widely-used example of this method. The NWI was established in 1974, with the goal of creating a national classification system (now known as the Cowardin 1979 system) and performing a fully inventory of the nation's wetlands and surface waters. The NWI originally used aerial imagery to delineate wetlands and surface waters by hand. As technology advanced, delineations are now done on computers, where the scale can be adjusted. Additionally, supplementary information, like soil surveys and topographic data, can be overlaid on the aerial imagery to aid with delineation decisions. Although still incomplete, the NWI is the largest database of identified wetlands in the nation (USFWS, 2020).

This method is far more efficient than field inventories and can clearly be applied at the regional scale, but comes at the cost of accuracy. An accuracy assessment of NWI wetlands in Pennsylvania as part of a research study by MacFaden et al. (2021), found that the NWI had an omission rate of 40.7 percent and a commission rate of 3.4 percent. Because of this, the NWI includes revisions based on field verifications, whenever they occur (USFWS, 1983). Additionally, this process requires manual analysis and still is not automated, making updating the inventory difficult.

2.4.3 Object-Based Image Analysis

Object-Based Image Analysis (OBIA) is a progressive method where pixels are grouped together based on their traits to form identifiable objects (Addink, 2010). Traditionally, pixels were identified individually, because image resolution was so coarse that each pixel accounted for a large portion of space. For example, the National Land Cover Database, first started in 1992, had a resolution of 30m. Although subsequent updates to this database have increased the efficacy range from 38-62 percent to 82-86 percent, small wetlands are generally not included (MacFaden et al., 2021; Addink, 2010; DiBiase et al., 2016; Jin et al., 2019).

Now that fine-resolution LiDAR data is available along with software that can easily combine multiple data sources, OBIA is a possibility. The same way our eyes identify objects by combining spectral (wavelength and color), shape, and neighborhood comparisons (e.g., size, color), GIS software works the same way to perform OBIA. Specific rules on categorization can be written into the GIS software, based on local knowledge of the AOI. For example, driveways could be differentiated from streets based on their size and relative location to houses (Addink, 2010).

MacFaden et al. (2021) ran a study to use OBIA to delineate wetlands within Pennsylvania, including FAVPs. They determined thirteen variables that influence wetland location (see Figure 3.13) and created statistical models to identify potential occurrences of wetlands. By combining layers of LiDAR DEMs, landcover data, climate data, aerial leaf-off orthoimagery (for spectral data), and soil data, wetlands were delineated with a tested accuracy of 81.5 percent. While the omission error was only 18.5 percent, the commission error was high at 15.6 percent.

2.4.4 Stochastic Depression Analysis

Originating in 2006, the Stochastic Depression Analysis (SDA) method uses an error probability function to account for inaccuracy in fine-resolution LiDAR data and delineate depressions in a more accurate manner (Lindsay & Creed, 2006). Since its development, different error function processes have been utilized. One of the most popular procedures is the

Monte Carlo approach. WhiteboxTools, a toolbox add-in to ArcGIS Pro, uses this approach in its SDA tool (Lindsay & Creed, 2005). First, a user specifies an error magnitude for the input raster DEM. A suitable error magnitude is the root-mean-square-error which can be found within the LiDAR metadata. This gives a standard deviation of error that the Gaussian error probability distribution function uses to establish a potential range of elevation values for each raster point. From there, the software randomly selects a value from each point's range to create a temporary DEM. Cells that are part of a depression are identified by a filling method—a DEM geoprocessing tool that raises elevations to remove depressions (see Appendix F)—and then placed on a list. This process gets repeated with new temporary DEMs for a specified number of iterations. If a cell has been placed on the list for more than a specified percentage of the iterations, it is denoted as belonging to a depression. Increased iterations lead to increased accuracy, but leads to an increased time cost (Wu et al., 2014).

Wu et al. (2014) took the WhiteboxTools SDA tool and designed a method to specifically delineate forested vernal pools, although the study was conducted in the non-Appalachian portion of Massachusetts. The SDA tool first delineated the depressions after an optimal number of fifty iterations. Then GIWs were selected by removing any depressions that were within a certain distance of waterways identified by the National Hydrography Dataset. Finally, they used the Normalized Difference Water Index parameter (an equation comparing proportions of reflected green light to infrared light that differentiates between water and soil/vegetation) in order to remove any depressions that did not have water present. Commission errors in the accuracy assessment ranged from 2-6 percent and omission errors were 8.2 percent. While the accuracy looks promising, this method has a heavy run-time that could be problematic for large regions and also is dependent on when the aerial flyovers occur.

2.4.5 Localized Contour Tree Delineation

Combining the knowledge that GIWs occupy depressional lows with the advent of high-resolution elevation data, Wu et al. (2015) developed localized contour tree delineation (LCTD), which uses depression contour lines (DCLs) to determine basins in much the same way traditional contour lines denote mountains. After drawing the DCLs, the software finds ‘seed contours’ which are closed contours that are surrounded by higher elevation DCLs—this is simply the reverse of how we find peaks on a mountain. Once a seed contour is found, the software looks for surrounding concentric closed DCLs until it reaches an open contour line (a contour line that does not form a closed loop within the map AOI) or until the surrounding closed DCLs are at lower elevations (which can occur when the GIW is a composite pool made of two separate depressions). The last closed contour before either of those two occurrences is considered to be the spill elevation (as long as the specified contour interval is small enough).

This spill elevation is a progressive modeling parameter that demonstrates recognition that GIWs are often hydrologically connected in high flow events. GIWs can fill, spill water over the basin edge, and merge with nearby GIWs to form a larger, singular basin. To track this, tree graphs are created for each group of depressions which show how contour lines fit within one another (see Figure 2.8) (Wu et al., 2015).

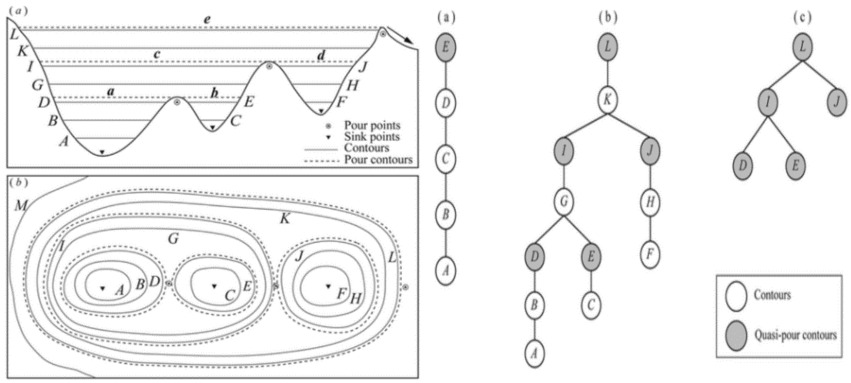

Figure 2.8 Localized Tree Contour Delineation diagram from (Wu et al., 2015)

Wu & Lane (2017) used LCTD to design a plugin toolbox for ArcGIS called the Wetland Hydrology Analyst Toolbox (WHAT) that was specifically designed for delineating GIWs in the Prairie Pothole Region and determining the flow paths between them. The delineations include an attribute table through which morphology measurements like surface area, perimeter, and volume can be obtained. The catchment area is also delineated for each GIW, as well as any flow paths that exist between it, other GIWs, and waterways. Because the study was more focused on hydrologic applications such as catchment area and flow path, no accuracy assessment was done with manual fieldwork or imagery analysis. Instead, the delineation results were compared to NWI delineations (see Figure 2.9). 59.2 percent of the NWI depressions were not delineated by the WHAT, the majority of these depressions being relatively small. Larger GIWs appear to be mapped with more success. The researchers stated that it was unknown whether the divergence between the NWI and the WHAT delineations were due to NWI error, WHAT error, land use changes, or differing data collection conditions.

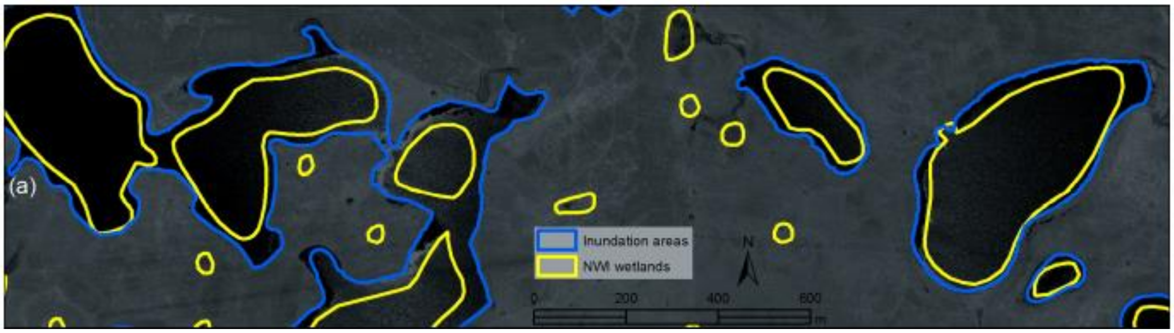

Figure 2.9 Delineation comparison of the Wetland Hydrology Analyst Toolbox and National Wetlands Inventory for a site in the Prairie Pothole Region of the United States from (Wu & Lane, 2017)

Chapter 3

Materials and Methods

3.1 Geology of the Northern Appalachian Ridges and Valleys

This thesis focuses on the Valley and Ridge physiographic province of the Appalachians, specifically the Northern Appalachian Ridges and Valleys region (see Figure 3.1), characterized by alternating ridges and valleys with trellis drainage features (USDA & NRCS, 2006).

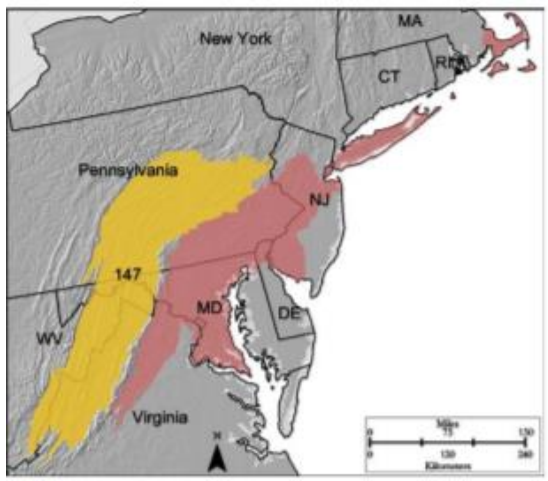

Figure 3.1 The Valley and Ridge province with the Northern Appalachian Ridges and Valleys region highlighted in yellow from (USDA & NRCS, 2006)

The Northern Ridges and Valleys is believed to have received major periglacial influences during the Wisconsin glacial stage (running approximately 75k-10k years ago). Periglacial influences include repeated freeze-thaw cycles and increased meltwater, both of which facilitate erosion (Clark et al., 1993). Figure 3.2 demonstrates a thought experiment on how erosion forms a valley between two ridgelines. Two columns of relatively erosion-resistant bedrock like sandstone (what will be the two ridgelines) have a section of more erosive lithology like shale (what will be the valley) between them. The shale has a small cap of sandstone, so originally the area can be considered level. The sandstone weathers, albeit slowly, so eventually the sandstone cap will erode away, exposing the shale below. From there, the shale erodes away at a far faster rate than the adjacent sandstone columns and the ridge and valley system develops.

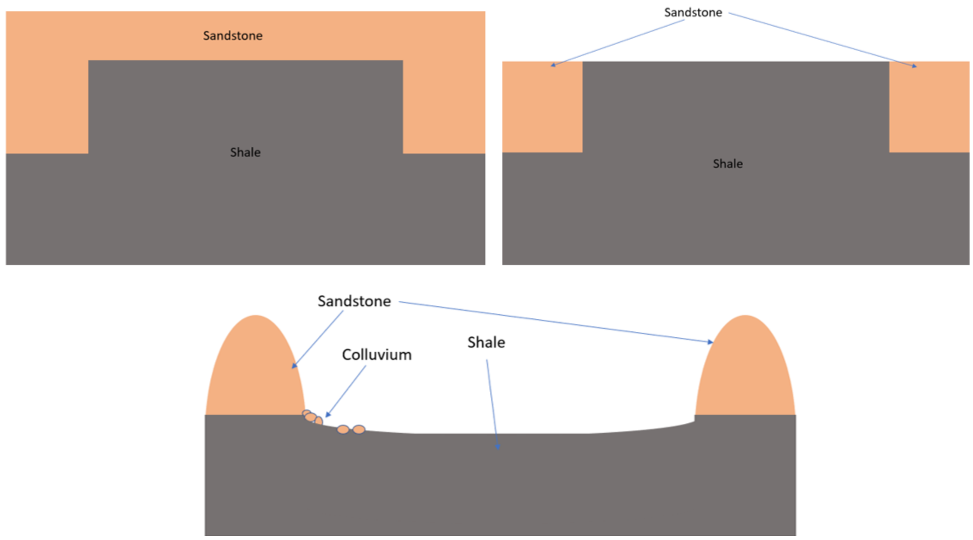

Figure 3.2 Formation of a ridge and valley system with initial stage (top left), erosion of the sandstone cap (top right), and formation of shale valley (bottom). Created in PowerPoint (Microsoft, 2021b)

Saddle formations are produced in a similar fashion to valleys. As the name suggests, saddles are saddle-shaped geologic formations either connecting two parallel ridgelines or connecting two peaks on the same ridgeline (see Figure 3.3). Saddles are characterized by having two opposing concave sides leading up to the ridgeline(s) and two opposing convex sides leading down into valleys or gaps. Because of their structure, saddles are capable of accumulating precipitation and dispensing streamflow. As such, they create very suitable conditions for FAVP formation and there are often several FAVPs per saddle (Blackman, 2019).

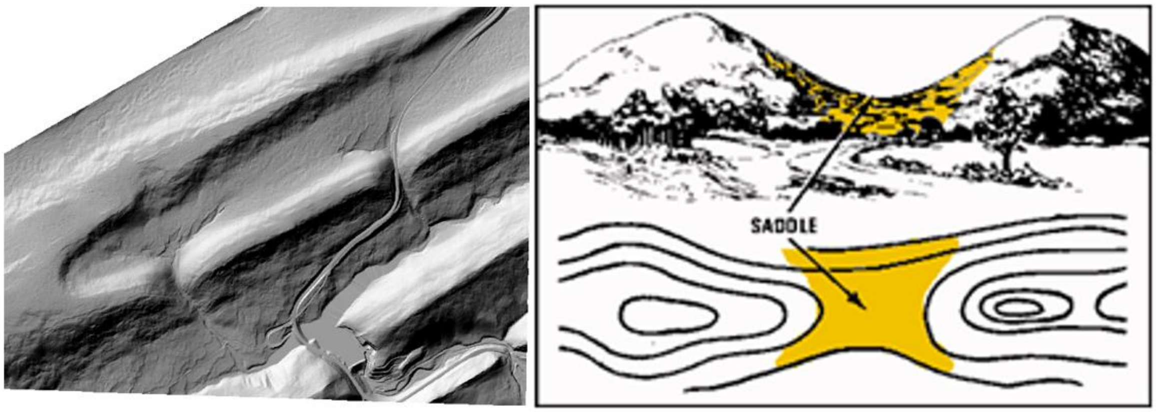

Figure 3.3 Saddles can either lie between two parallel ridgelines (left) or connect two peaks in the same ridgeline (right). Left DEM created from LiDAR data from (PADCNR, 2006-2008) in ArcGIS Pro (Esri, 2021a). Right image from (Khan, 2020)

3.2 Site Description

The selected site for this thesis is an Appalachian Ridge and Valley saddle landscape along the Rothrock State Forest Ben Jacobs Trail (BJT) in Mifflin County. Connecting two Tuscarora sandstone ridgelines to the north and south, the Juniata shale saddle drops off to the east towards US Route 322 and to the west towards Muttersbaugh Gap (see Figure 3.4) (PADCNR, 2001). This saddle will hereby be referred to as the BJT.

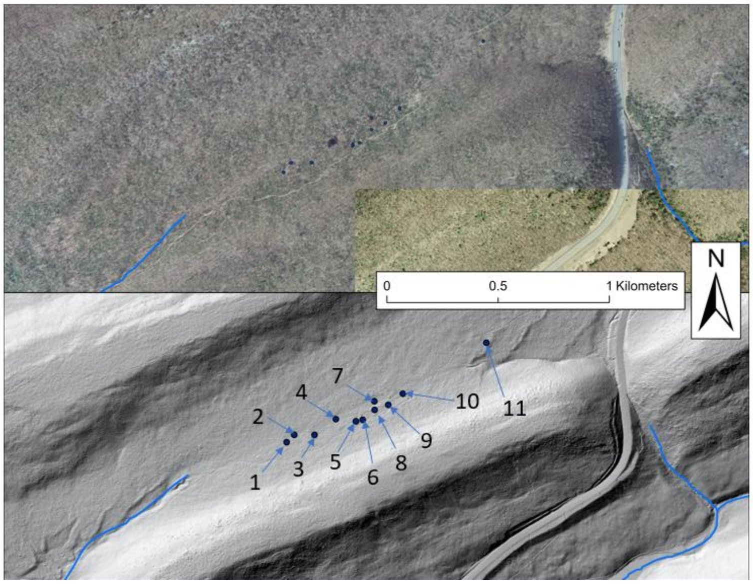

Figure 3.4 Ben Jacobs Trail saddle area with eleven forested Appalachian vernal pools. Aerial and Hillshade imagery from (PASDA, 2021). Pool and stream delineations and map creation courtesy of Taylor Blackman in ArcGIS Pro (Esri, 2021a). Labeling created in PowerPoint (Microsoft, 2021b)

3.2.1 Site Hydrology

The BJT has a total of eleven FAVPs (see Figure 3.4). The saddle center is the lowest and flattest part of the formation, collecting the most surface and subsurface flow from the surrounding ridgelines and so is where ten of the eleven pools are found. The eleventh pool is located on the eastern end of the saddle on the edge of a solifluction lobe. Solifluction lobes are a geologic formation formed under periglacial or glacial conditions. The repeated freeze-thaw cycles weaken the soil on slopes, causing their surfaces to collapse and slide downhill. Solifluction lobes appear on LiDAR hillshade maps as wrinkles on hillsides (see Figure 3.5). Because each wrinkle creates a knickpoint, FAVPs can be found uphill of solifluction lobes (Blackman, 2019).

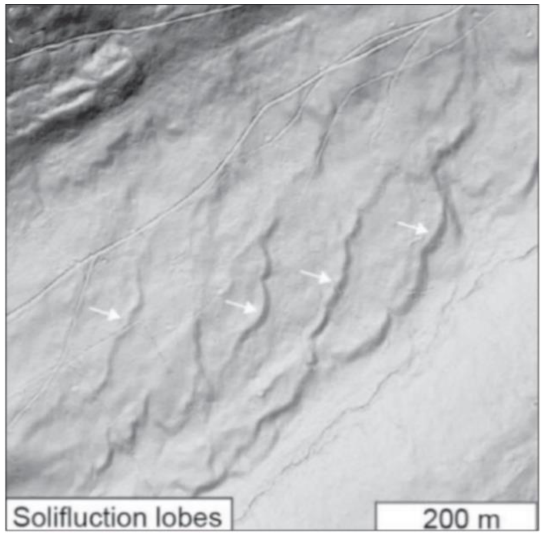

Figure 3.5 Solifluction Lobes from (DiBiase et al., 2017)

Figure 3.4 shows the numbering system used to discuss the pools. Pools 1 and 2 are mid-sized and under dry conditions are separate. However, under high flow events, the middle section will become inundated to form a singular arc-shaped pool. Even under drier conditions, the middle section can be saturated. Pools 4 and 7 are the largest pools in the saddle and both resemble a true marsh with a majority surface area covering of hydrophilic tall grasses. Pools 5 and 10 also have portions of their surface area covered by a grass species, but still have a significant amount of unvegetated space. Pools 6 and 8 are the second smallest and smallest pools, respectively. Pool 11 is a solifluction pool and so characteristically is smaller in size. Table 3.1 shows drone imagery of these eleven pools.

Table 3.1 Drone imagery of eleven Forested Appalachian Vernal Pools (scale not uniform) and Pool 1+2 connection from (Blackman, 2020)

1 	2 
3 	4 
5 	6 
7 	8 
9 	10 
11 	1+2 

If the FAVPs are the collection mechanism of flow for the BJT, then the convex ends of the saddle are the conveyance mechanism. The eastern end of the saddle has a defined dry channel that likely fills in high-flow events and that connects with a stream that runs parallel with US Route 322 (see Figure 3.6). On the western end of the saddle, five sumps release groundwater to the surface, which combines with a rising water table to create a headwater stream that runs down Muttersbaugh Gap (see Figure 3.6).

Figure 3.6 Stream systems in the BJT saddle. From left to right: Dry channel on eastern end, locations of sumps on western end, one of the five sumps, and headwater stream on western end. Original LiDAR data from (PADCNR, 2006-2008). DEM created in ArcGIS Pro (Esri, 2021a) and edited in PowerPoint (Microsoft, 2021b)

3.2.2 Site Geology

There are significant portions of Muttersbaugh Gap where the headwater stream, leaving the western end of the BJT, becomes concealed by large amounts of colluvium (see Figure 3.7). Colluvium is rocky material that is largely transported by gravity. Colluvial deposits range from dense sand to large boulders (Parry, 2011). The source of the colluvium in the BJT and Muttersbaugh Gap is from the Tuscarora sandstone ridgelines. Sandstone is less erosive than shale, but often more easily fractured (Senseny & Pfeifle, 1984). As a result, chunks of sandstone can break off the ridges, and because gravity is the major vehicle of transport, the aspect of the ridgeline determines where the colluvium ends up. The north ridgeline of the BJT is angled towards the saddle center, so colluvium is directed down towards the BJT. The south ridgeline, however, is angled away from the saddle center, so colluvium is directed off the backside. Part of this backside coincides with the eastern edge of the gap and so a boulder field is formed on that side (see Figure 3.8).

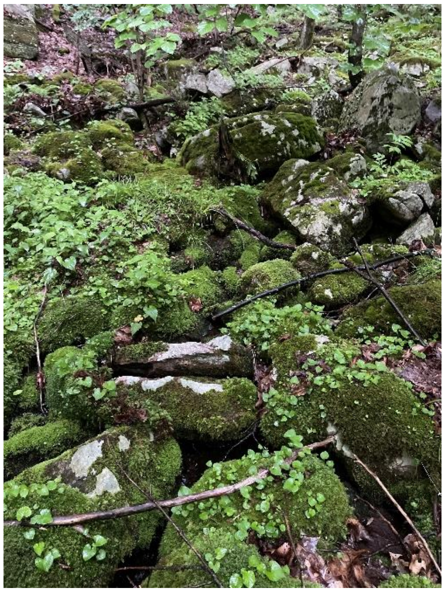

Figure 3.7 Concealment of western BJT headwater stream by colluvium

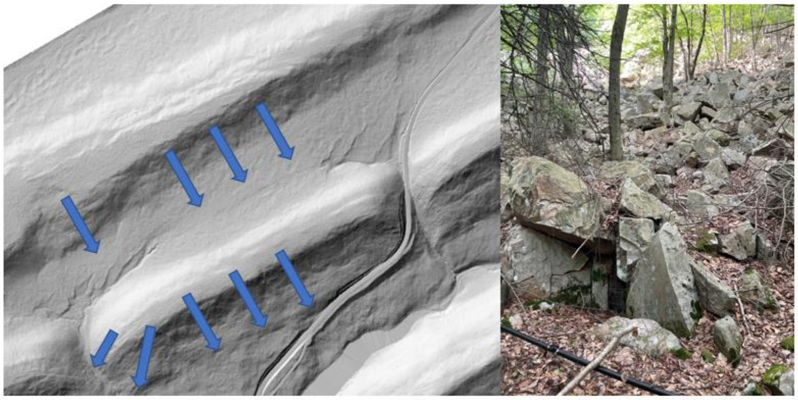

Figure 3.8 Direction of colluvium (left) and colluvium in gap (right). Original LiDAR data from (PADCNR, 2006-2008). DEM created in ArcGIS Pro (Esri, 2021a) and edited in PowerPoint (Microsoft, 2021b)

Since the majority of colluvium is coming from the north ridgeline, the northern half of the saddle center has the highest density of boulders, while the pools are located just south of them. Colluvium can affect formation of FAVPs by diverting flow or by creating enough porous space for groundwater tables to sink deeper. Colluvium also makes mapping efforts very difficult since it creates obstacles for fieldwork, conceals flow for aerial imagery analysis, and creates spurious depressions for LiDAR methods. Its influence on the WHAT is therefore unknown.

3.3 Study Procedure and Metadata

To test the accuracy of the WHAT delineation, manual measurements were taken or calculated for perimeter, surface area, length, and width. These measurements were compared to the respective outputs of the WHAT, local knowledge imagery analysis (LKIA), NWI, and OBIA. All measurements were recorded in meters—meters squared for surface area—to at least one decimal. Identification success was also recorded to see how many pools were delineated by each method.

3.3.1 Wetland Hydrology Analyst Toolbox

The WHAT was treated largely as a black box, due to differences in the description of the toolbox in the Wu & Lane (2017) paper, in the YouTube tutorial video of the toolbox (found on the WHAT public GitHub page), and in the toolbox itself once downloaded. Both the paper description and tutorial video appeared to be for an earlier or different version of the toolbox. They showed only three tools with some differences in inputs.

The WHAT was downloaded for free from the public GitHub page: https://github.com/giswqs/Wetland-Hydrology-Analyst-Toolbox. The WHAT is written in Python 2, so it was opened in ArcMap 10.8 (Esri, 2021b). The WHAT has a total of four tools: Extract Sink, Identify Depressions, Delineate Catchments, and Delineate Flowpaths. Only the first two tools were used for this thesis. Figure 3.9 shows the input parameters for each tool. To determine optimal parameters for FAVP delineation, the first part of this thesis involved experimenting with different inputs. For both tools, any numeric parameter was tested with incremental values and the same 2006 DEM, while DEM parameters were tested with different DEMs.

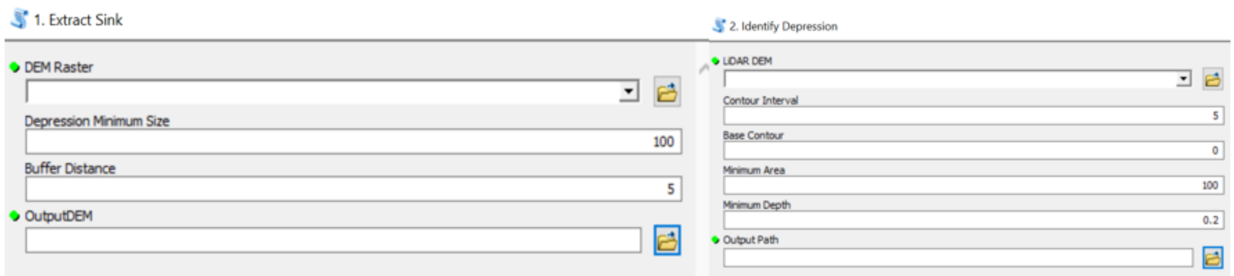

Figure 3.9 Parameters for Extract Sink and Identify Depressions tools with default values from (Wu & Lane, 2017) toolbox opened in ArcMap (Esri, 2021b)

DEMs were sourced from the public Pennsylvania Spatial Data Access (PASDA) database, where raw LiDAR data and pre-made DEMs can be directly downloaded. The first DEM was created in ArcGIS Pro 2.8 (Esri, 2021a) from LiDAR point cloud data produced through the 2006-2008 PAMAP Program. Collected in the spring of 2006 (late March to May), the DEM raster data have a horizontal ground resolution of 3.2 feet and were in the 'NAD1983 StatePlane PA South FIPS 3072 (US feet)' projection coordinate system (PADCNR, 2006-2008). In order to encompass the whole AOI, multiple DEMs had to be combined into a singular DEM with the Mosaic to New Raster tool. The second, pre-made DEM was produced through the South Central Pennsylvania 2017 QL2 LiDAR project. Collected in the late fall of 2017 (late November to late December), the DEM raster data have a nominal pulse spacing of 0.7 meters and were in the 'NAD 1983 (2011) UTM Zone 18N' projection coordinate system (USGS, 2017). It was only necessary to download one DEM. Appendices D and E provide in-depth tutorials on downloading, creating, and geoprocessing DEMs from PASDA. Both the 2006 and 2017 DEMs were used as inputs for Extract Sink and Identify Depressions in order to create a time comparison.

Each tool in the WHAT produces' multiple outputs (see Figure 3.10). Since the Extract Sink tool creates multiple DEM outputs, these were included as possible inputs for the Identify Depressions DEM parameter, along with the raw 2006 and 2017 DEM. Table 3.2 illustrates all the different experimental parameter inputs for the two tools.

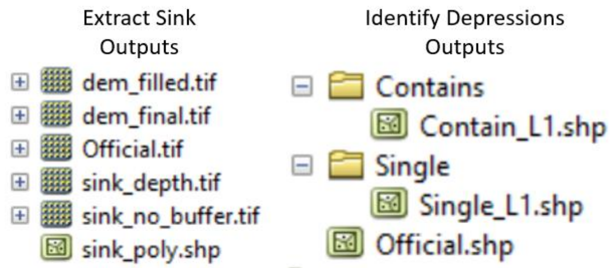

Figure 3.10 Extract Sink (left) and Identify Depressions (right) outputs from (Wu & Lane, 2017) toolbox used in ArcMap (Esri, 2021b). The specified input name is 'Official' to identify the official return

Table 3.2 Experimental inputs for Extract Sink and Identify Depressions

Extract Sink

DEM Raster	Depression Min. Size	Buffer Distance	Using 2006 Metric DEM up until Time Comparison
Metric 2006	1	0	
Pasda 2017	10	0.1	
	50	1	
	100	5	
		10	
		100	

Identify Depressions

Lidar DEM	Contour Interval	Base Contour	Min. Area	Min. Depth	Using Contains/Single shapefiles and 2006 Metric DEM up until Time Comparison
Metric 2006	1	0	25	0	
ES-100-1 Final	3	1	50	0.1	
ES-100-100 Final	5	7	75	0.2	
ES-100-100 No Buffer	10	10	100	0.5	
ES-100-1 Official	50	100		1	
Pasda 2017					
Pasda 2017 ES-100-1 Official					

Table 3.3 shows the parameters that were deemed optimal for the delineation comparison. The resultant optimal delineation shapefile was moved to ArcGIS Pro. Of the ten returned

depressions for the DEM, only those depressions located within the saddle AOI were moved onto a new layer, as well as the Laurel Run small reservoir south of the AOI.

Table 3.3 Thesis-Optimal parameters for Extract Sink and Identify Depressions

Extract Sink

DEM Raster	Depression Min. Size	Buffer Distance
PASDA 2017	100	1

Identify Depressions

Lidar DEM	Contour Interval	Base Contour	Min. Area	Min. Depth
Pasda 2017 Official ES-100-1	1	0	50	0.2

3.3.2 Manual Fieldwork Measurements

Manual measurements were taken with a combination of a 100m measuring tape and a 300ft measuring tape. Conversions were made to meters and all measurements were made to at least one decimal place. The maximum perimeter of each pool was measured, using hydrologic indicators employed by the US Army Corps of Engineers like blackened leaves, moss lines, and any knickpoints at the lip of the depression (Stevens, 2011). Also used to identify upland was encroaching mountain laurel, a facultative upland species. Assuming the pools most closely resemble ovals in shape, the major axis was measured and recorded as the length, while the minor axis was measured and recorded as the width. Surface area was calculated by assuming that pools were oval in shape and so using the equation: ½ major axis * ½ minor axis * π. This calculation cannot be considered wholly accurate because of its generalizing assumption.

Pool 5 was measured at the beginning of August. Pools 3 and 8-11 were measured the first week of September, and Pools 1-2 and 4-7 were measured the second week of September.

This was due to limited available time to get out to the site as well as an equipment malfunction with the measuring tape. The temporal gap should not affect the results since measurements were taken as maximums and the hydrologic indicators do not change within the span of a month.

Because Pools 1 and 2 are combined by the WHAT but not by other methods, Pool 1, Pool 2, and the section between them (Pool 1-2) were measured both individually and combined (Pool 1+2). Pool 1+2 cannot be treated as an oval due to its arc shape, so the surface areas of Pool 1, Pool 2, and Pool 1-2 were summed instead.

3.3.3 Local Knowledge Imagery Analysis

Taylor Blackman is a Ph.D. student at the Pennsylvania State University conducting FAVP research in the same AOI as this thesis, so he provided manual digitization of the pools using LiDAR hillshade and aerial imagery. This method of delineation is much the same as the NWI process, but differs in that Taylor was able to verify and modify each delineation based on local knowledge gained in the field. Therefore, this delineation can be considered the second most accurate dataset for the other methods to be compared against. The original projection coordinates for the shapefile were in 'NAD 1983 StatePlane Pennsylvania South FIPS 3702 (US Feet)'.

3.3.4 National Wetlands Inventory

The NWI dataset will represent the aerial imagery analysis methodology, and the term NWI will hereby be synonymous with that method. The NWI used May 1983 color infrared aerial imagery at a scale of 1:58,000 to delineate the FAVPs in the BJT. Delineation was based on observable vegetation, hydrology, and topography (USFWS, 1983). Because of the FAVPs' remote location and small size, it is unlikely these pools had fieldwork verifications performed.

The entire NWI dataset for Pennsylvania, containing all wetlands and surface waters, was downloaded and opened in ArcGIS Pro, but only the FAVPs within the BJT were moved onto a new layer, as well as the Laurel Run small reservoir south of the BJT. The original projection coordinates for the resultant shapefile were in 'NAD_1983_Albers'.

3.3.5 Object-Based Imagery Analysis

The Modeled Primary Wetlands dataset for Pennsylvania produced by MacFaden et al. (2021) will represent the OBIA methodology for this thesis. The thirteen variables used in the study and their respective data sources can be viewed in Table 3.4. Predictive wetland maps, created using quantitative variables like climate data and topography, were combined with a rule-based OBIA, using qualitative variables like land cover type and image characteristics (e.g., color, pattern, shape) to delineate the wetlands. Finally, some delineation adjustments were applied to improve quality and accuracy. The full process outline is shown in Figure 3.11. Although the study paper was published in 2021, the dataset is considered as relevant to 2013.

Table 3.4 MacFaden et al. (2021) table of thirteen variables used in the study and their data sources

Variable	Source	Scale or resolution (m2)	Original units	Climate down-scaling	Terrain modeling variable	Object-based mapping
Elevation (DEM)	LiDAR and PRISM Climate Group	1, 3, 10, and 800	Feet	x	x	x
nDSM	Calculated from LiDAR and DEM	1	Feet			x
LiDAR intensity	Calculated from LiDAR	1	Feet			x
Latitude and longitude		10 and 800	Feet	x		
Aspect		10 and 800	Degrees	x		
Slope			Degrees			
Dissection	Calculated from DEM	10	Index		x	
Exposure			Index			
CTI	Calculated from DEM	3 and 10	Index		x	x
Clim_pc1 (first PCA axis, climate)	Downscaled from PRISM Climate Data	10	Index	x	x	
Mean temperature (T_{mean})	PRISM Climate Group: Long-term Normals 1980 to 2010	800	Degrees celsius	x		
Maximum temperature (T_{max})						
Minimum temperature (T_{min})						
Dew point temperature (T_{dmean})						
PPT			Millimeter		x	
Land-cover data	2013 Statewide	1	Presence–absence			x
Soil types	SSURGO	Various	Categorical		x	
Leaf-off aerial orthoimagery	PAMAP Program True-color Orthophotos, 2005 to 2008	0.3	Meters			x

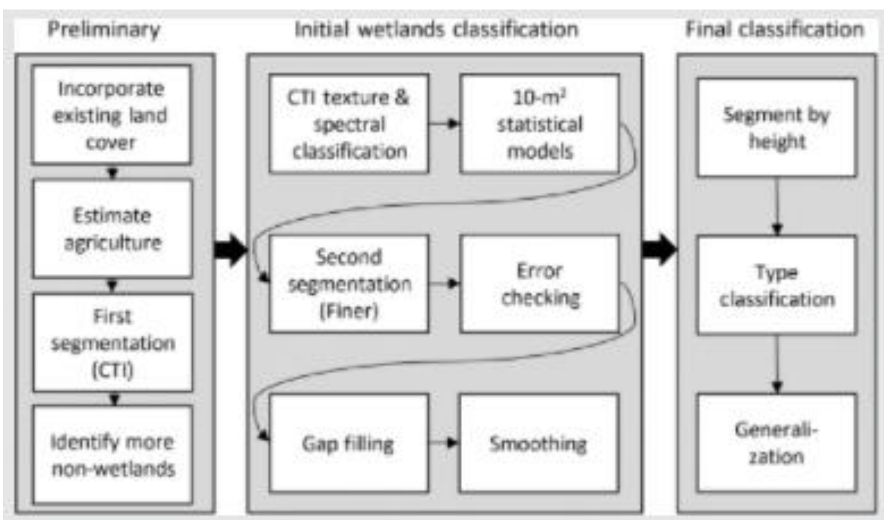

Figure 3.11 MacFaden et al. (2021) diagram of study workflow

The dataset is a combination of specific small pool delineations and a large area delineation that encompasses several pools. These large delineations often encompass lots of area that has no pools (see Figure 3.12). For the purpose of morphology comparison and identification success, only the specific pool delineations shapefile was opened in ArcGIS Pro. Only those depressions located within the saddle AOI were moved onto a new layer, as well as the Laurel Run small reservoir south of the AOI. The original projection coordinates for the resultant shapefile were ‘Albers Conical Equal Area’.

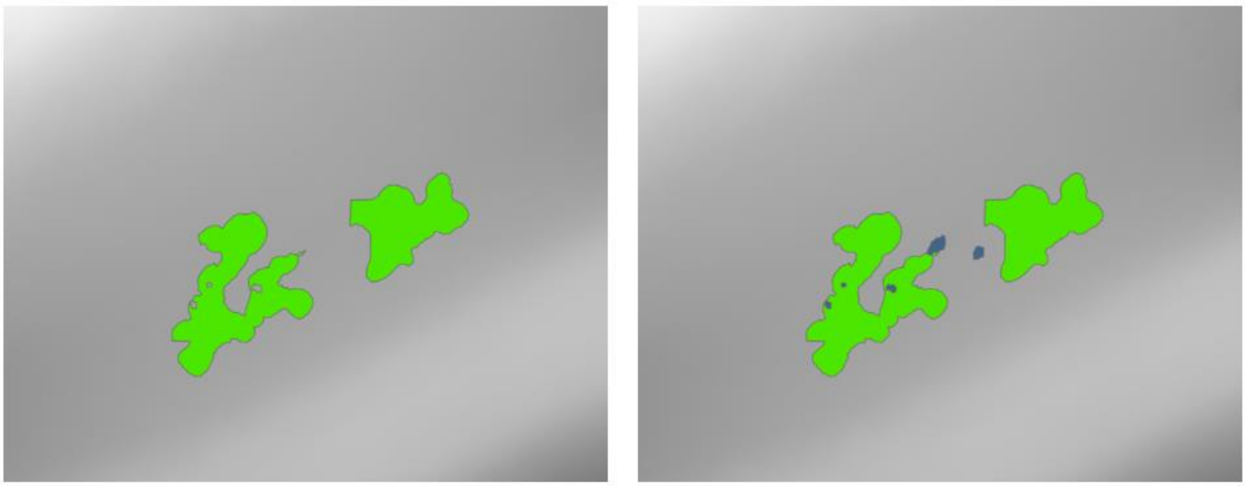

Figure 3.12 General MacFaden et al. (2021) delineation without (left) and with (right) specific delineation. DEM (USGS, 2017) viewed in ArcGIS Pro (Esri, 2021a)

3.4 Data Processing and Analysis

Upon being added to ArcGIS Pro 2.8 (Esri, 2021a), each method delineation shapefile was projected (if necessary) with cubic interpolation to ‘NAD 1983 (2011) UTM Zone 18N’. Distance was preserved at the expense of preserving shape.

Perimeter and Surface Area were calculated with the Calculate Geometry tool and added as fields to each shapefile’s attribute table. Length and Width had to be calculated by use of the Measure Tool. The span closest resembling a major axis was the length, while the span closest resembling a minor axis was the width. The measurements data was all moved into an Excel (Microsoft, 2021a) file.

Identification success for each method was determined by the number of omission errors (LKIA had a pool, but no pool was delineated by method) and the number of commission errors (LKIA did not have a pool, but a pool was delineated by method).

Morphology delineation comparison was determined by calculating percent error for each of the four measurements between each method (NWI, OBIA, and WHAT) and the manual measurements. The same was done for the LKIA measurements to be used as a modeled delineation benchmark for accuracy. Percent errors were recorded to two decimals. Finally, the average error was calculated for each method for each of the four measurements and the results were compared.

Chapter 4

Results and Discussion

4.1 Wetland Hydrology Analyst Toolbox Tools

Due to its scripts being in Python 2, the WHAT requires ArcMap (Esri, 2021b) to run. This is unfortunate, since ArcMap is more cumbersome and slower in runtime than ArcGIS Pro, which accepts Python 3 script. Because the full tool scripts can be found on the WHAT GitHub page, the translation from Python 2 to 3 is fully possible. It is made easier by the presence of the Python translator utility ‘2to3’, which can be used as a conversion starting point (Esri, n.d.-h).

The numeric input units are confirmed to be in the metric system, after experimenting with parameter values and comparing to values obtained with the Measure tool in ArcMap.

4.1.1 Extract Sink

Table 4.1 shows the results of the iterative parameter test, using a 2006 PASDA DEM (see Appendix A for raw results). The ‘Depression Minimum Size’ parameter determined the number of sinks that were found, with larger minimum sizes producing less sinks. A minimum size of 100 sq. meters extracted the same number of BJT pool sinks as a minimum size of one sq. meter, with far less extraneous sink noise (see Figure 4.1) and with a much faster runtime. These reasons made 100 sq. meters the optimal ‘Depression Minimum Size’ parameter for the delineation comparison.

Table 4.1 Extract Sink Parameter Test Results

DEM Raster	Test ID	Depression Min. Size	Buffer Distance	# Sinks
Metric 2006 Test	1	100	0	173
	2	100	0.1	173
	3	100	10	173
	4	100	100	173
	5	1	1	12739
	6	10	1	3835
	7	100	1	173
	8	50	1	479
	9	100	5	173

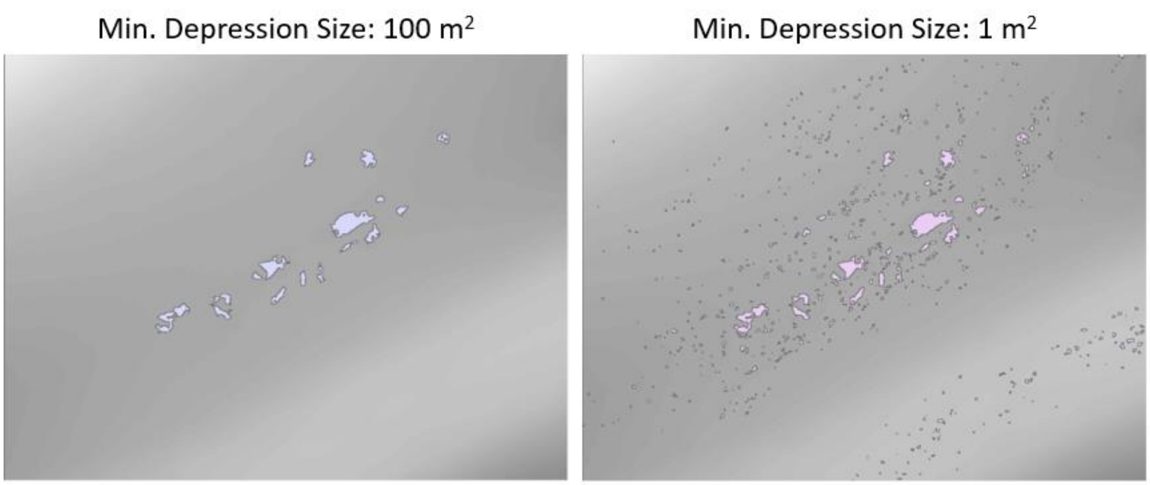

Figure 4.1 Extract Sink return with Minimum Depression Size of 100 sq. meters (left) and 1 sq. meter (right). DEM (PADCNR, 2006-2008) viewed in ArcMap (Esri, 2021b)

The ‘Buffer Distance’ parameter relates to the localized contour tree delineation method. For large contour intervals, there can be a difference between the true pour contour and the pour contour that is determined (the true pour contour exists between two contour lines). A buffering algorithm (which can take a buffer size parameter) can therefore be used to move the calculated pour contour closer to the true pour contour (Wu et al., 2015). Buffering is often not necessary for small contour intervals. Some intermediate outputs of the tool depict a comparison of different buffer sizes (see Figure 4.2). The ‘Buffer Distance’ parameter did not seem to affect the output at all, but was not allowed to be zero meters. An arbitrary value of one meter was used for the buffer size.

Figure 4.2 A buffer of 100 (yellow circle) versus a buffer of 1 (not visible) for a sink (green). DEM (PADCNR, 2006-2008) viewed in ArcMap (Esri, 2021b)

The Extract Sink tool produces six outputs: five .tif files and a shapefile of the extracted sinks (see Figure 3.10). The output that gets added to the ArcMap Table of Contents pane is the .tif file that receives the name specified as an input. For this reason, it will hereby be referred to as the 'official' output. The remaining .tif files required estimated guesses to understand their uses. 'dem_filled.tif' most likely is the official output after it has been preprocessed with a filling technique, effectively removing the depressions (see Appendix F for a tutorial on filling and breaching geoprocessing methods). It is unknown which type of fill geoprocessing method was used. 'sink_depth.tif' most likely can be used as an input in the Delineate Catchment or Delineate Flow Path tools. 'sink_no_buffer.tif' likely does not include the buffer size information, but both it and 'dem_final.tif' (unknown difference) are able to be used as inputs for the Identify Depressions tool.

4.1.2 Identify Depressions

Table 4.2 shows the results of the iterative parameter test (see Appendix B for raw results). The included Extract Sink .tif outputs originally used the 2006 PASDA DEM as their Extract Sink input. The ‘ES-100-100 No Buffer’ identified fewer depressions in the DEM and in the BJT compared to the ‘ES-100-100 Final’, demonstrating the value of using a buffer-containing DEM. However, the total match in results between ‘ES-100-100 Final’ and ‘ES-100-1 Final’ indicates that the value of the buffer does not matter. The raw 2006 PASDA DEM (‘Metric 2006’) produced rounder, more full depressions, and identified more depressions than ‘ES-100-1 Official’ when both were using the same contour interval. However, because ‘ES-100-1 Official (CI 1)’ can use a contour interval of one meter and ‘Metric 2006’ cannot, the former can identify more depressions, even if they are not as rounded-out.

Table 4.2 Identify Depressions parameter test results

Test ID	Lidar DEM	Contour Interval	Base Contour	Min. Area	Min. Depth	# Sinks	Depressions (not Pools) in Saddle
Change Depth							
1	Metric 2006	5	0	50	0	27	3
2	Metric 2006	5	0	50	0.1	27	3
3	Metric 2006	5	0	50	0.2	27	3
4	Metric 2006	5	0	50	0.5	26	3
5	Metric 2006	5	0	50	1	26	3
Change Area							
6	Metric 2006	5	0	25	0.2	28	3
7	Metric 2006	5	0	50	0.2	27	3
8	Metric 2006	5	0	75	0.2	24	3
9	Metric 2006	5	0	100	0.2	21	2
Change Base							
10	Metric 2006	5	0	50	0.2	27	3
11	Metric 2006	5	1	50	0.2	39	1
12	Metric 2006	5	7	50	0.2	32	1
13	Metric 2006	5	10	50	0.2	27	3
14	Metric 2006	5	100	50	0.2	27	3
Change Int.							
15	Metric 2006	1	0	50	0.2	932	9+
16	Metric 2006	3	0	50	0.2	~50	0
17	Metric 2006	5	0	50	0.2	27	3
18	Metric 2006	10	0	50	0.2	11	1
19	Metric 2006	50	0	50	0.2	4	0
Change DEM							
20	Metric 2006	5	0	50	0.2	27	3
21	ES-100-1 Final	5	0	50	0.2	21	2
22	ES-100-100 Final	5	0	50	0.2	21	2
23	ES-100-100 No Buffer	5	0	50	0.2	8	1
24	ES-100-1 Official	5	0	50	0.2	21	2
25	ES-100-1 Official (CI 1)	1	0	50	0.2	87	4

'Contour interval' largely determines the number of identified depressions, both in the BJT and in the whole DEM. Smaller contour intervals identify more depressions, but have an exponentially greater runtime. The tool can become so memory intensive that it causes ArcMap to stop responding. This happens with the 'Metric 2006' DEM, because it is a large amount of area for the tool to analyze so closely. Running those parameters for an entire region would therefore not be possible. The Extract Sink tool rectifies this issue by decreasing the DEM area down to just potential depressions (see Figure 4.3), thus allowing for intensive analysis by the Identify Depressions tool. Although smaller contour intervals identify more depressions, that does not necessarily mean they will identify more saddle depressions. For example, a contour interval of three meters identifies fewer depressions in the BJT than a contour interval of five meters. It is unknown why this occurs, but contour intervals of one and five meters seem to be productive, with one meter being optimal.

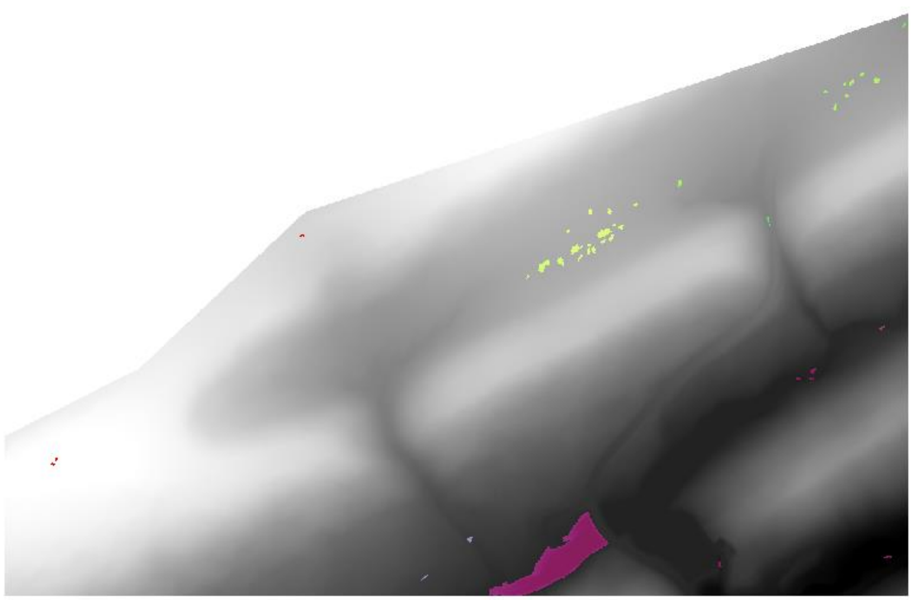

Figure 4.3 Extract Sink official output DEM (colored) on original PASDA 2017 DEM (USGS, 2017). Viewed in ArcGIS Pro (Esri, 2021a)

The ‘Base Contour’ parameter seems to follow an odd pattern. Inputs of 0, 10, and 100 meters all produce the same results. However, seven meters identifies more depressions (although less in the BJT), while one meter identifies even more. Additionally, both one and seven meters delineate a single FAVP not identified by any of the other iterations—Pool 6 and Pool 9, respectively. The base contour is used as a starting point for the contour lines (Wu et al., 2015) and so seems to work in tandem with the contour interval to majorly influence which depressions are identified. However, more research is needed to understand exactly how this parameter influences delineation. A preliminary optimal value of zero meters was used for this thesis, since it identified the most depressions within the BJT.

The Identify Depressions tool produces three distinct outputs (see Figure 3.10). The ‘official’ output that receives the specified input file name is a shapefile that does not delineate the depressions, but rather delineates the surrounding ridgelines. There are areas where the shapefile delineations overlap with the delineated depressions (see Figure 4.4). The remaining two outputs are folders named ‘Contains’ and ‘Single’. Within these folders are shapefiles that both delineate the same identified depressions. Using a contour interval of three meters creates an output with the depressions split between two ‘Contains’ and two ‘Single’ files. There are no discernable differences between the ‘Contains’ shapefiles and the ‘Single’ shapefiles, and either one produces the desirable delineated depressions output.

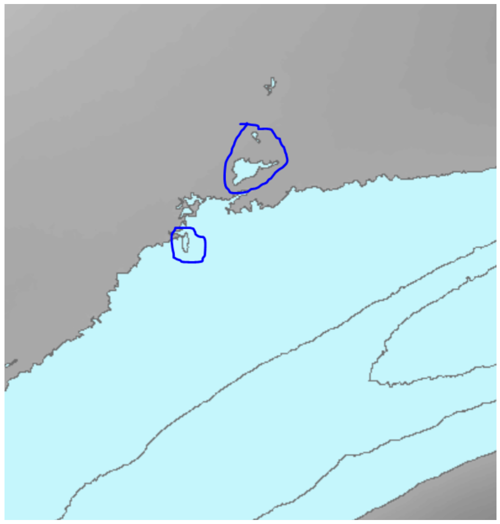

Figure 4.4 Identify Depressions official output (ridgeline) with circled areas where Contains/Single depressions exist. DEM (PADCNR, 2006-2008) viewed in ArcMap (Esri, 2021b) and edited in Excel (Microsoft, 2021a)

4.1.3 Pennsylvania Spatial Data Access DEM Time Comparison

For both the Extract Sink and Identify Depressions tools, using the 2017 PASDA DEM greatly improved the data quality compared to using the 2006 PASDA DEM (see Figure 4.5). The sinks and depressions were more rounded-out and more depressions were identified within the BJT. However, this only occurred when using the official output DEM of the Extract Sink (which in turn used the raw 2017 DEM input). When the raw 2017 PASDA DEM was used as an input to the Identify Depressions tool, no saddle depressions were found.

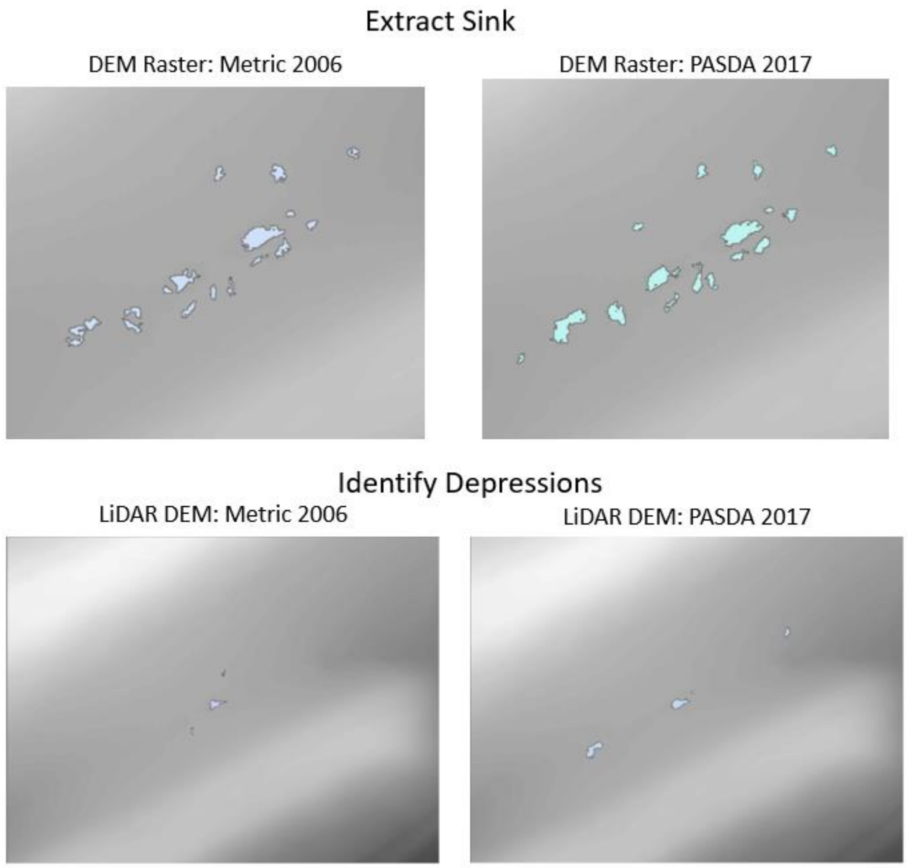

Figure 4.5 Time Comparison between 2006 and 2017 LiDAR data for Extract Sink and Identify Depressions tools. DEMs (PADCNR, 2006-2008; USGS, 2017) viewed in ArcMap (Esri, 2021b) and edited in PowerPoint (Microsoft, 2021b)

It is not surprising that the 2017 DEM is better than the 2006 DEM. As LiDAR data improves in accuracy and the number of spurious artifacts in the DEM decreases, features are able to be delineated more accurately. The automated ability of the WHAT allows for regional databases to be almost immediately updated when new datasets are released.

4.2 Delineation Methods Identification Success (Commissions and Omissions)

Figure 4.6 shows the delineations of each of the modeling methods next to the LKIA for reference. Each method had a high number of omission errors (see Table 4.3) with the OBIA identifying one more FAVP than the NWI and the WHAT. The WHAT was the only method to have a commission error, located northeast of Pool 7. This depression has a surface area of 100 sq. meters, which is at least twice as large as Pool 8. By looking at a hillshade DEM, a scar is present, however there also exist scars north of Pool 7 that were not delineated (see Figure 4.7). Likely, the colluvium that collects on the northern end of the saddle center forms depressions, but no water collects nor does the water table break the surface. Why the WHAT delineated that one depression versus the others is unknown.

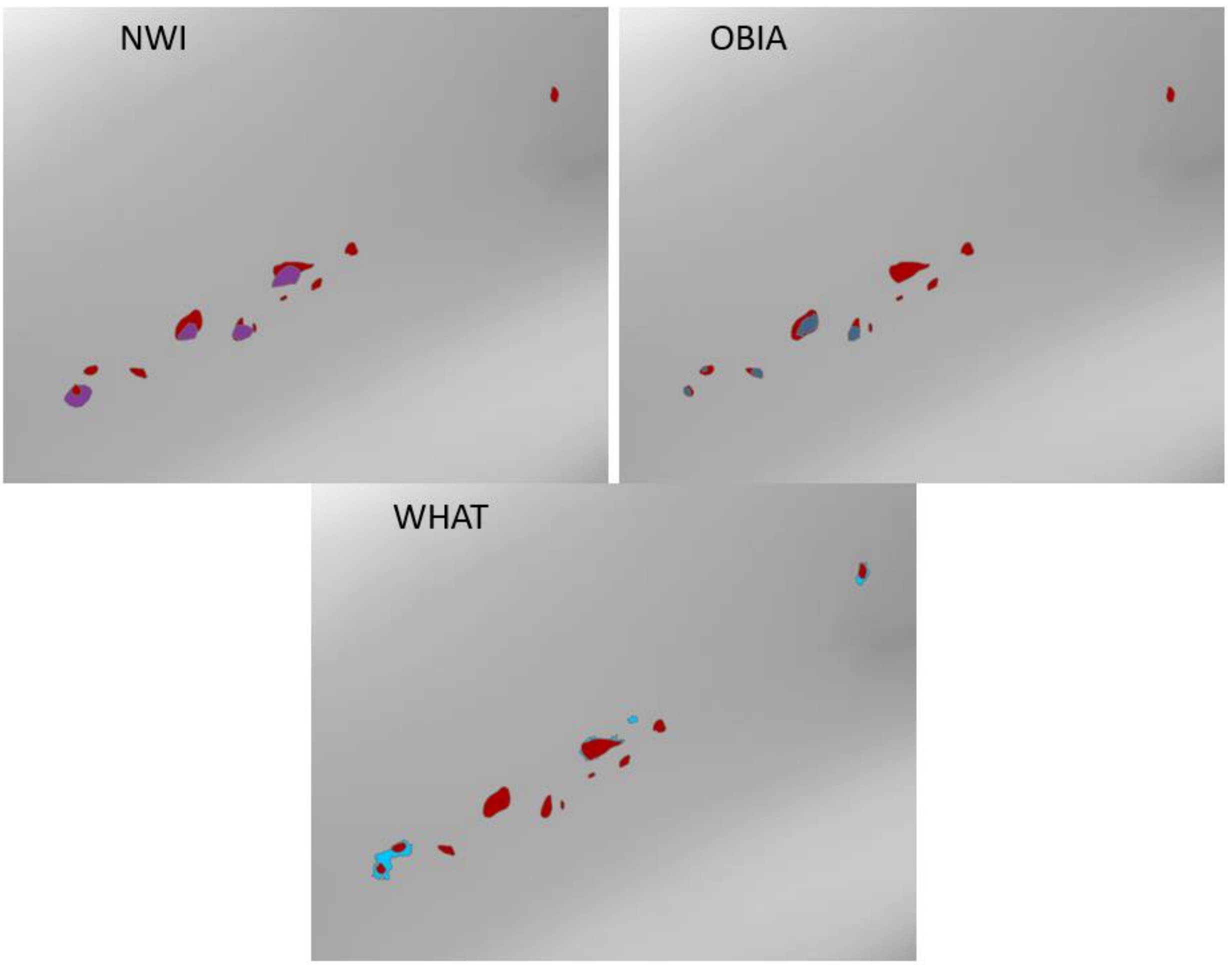

Figure 4.6 Delineations for the three modeling methods compared to the Local Knowledge Imagery Analysis delineations (red). Note: For the NWI comparison, the Pool 1 LKIA delineation was moved on top of the NWI delineation for better viewing. DEM (USGS, 2017) viewed in ArcGIS Pro (Esri, 2021a)

Table 4.3 Commission and Omission Errors for each of the delineation methods

	True Id.	Omission Errors	Commissions Errors
Manual	11	0	0
NWI	4	7	0
OBIA	5	6	0
WHAT PASDA 2017	4	7	1

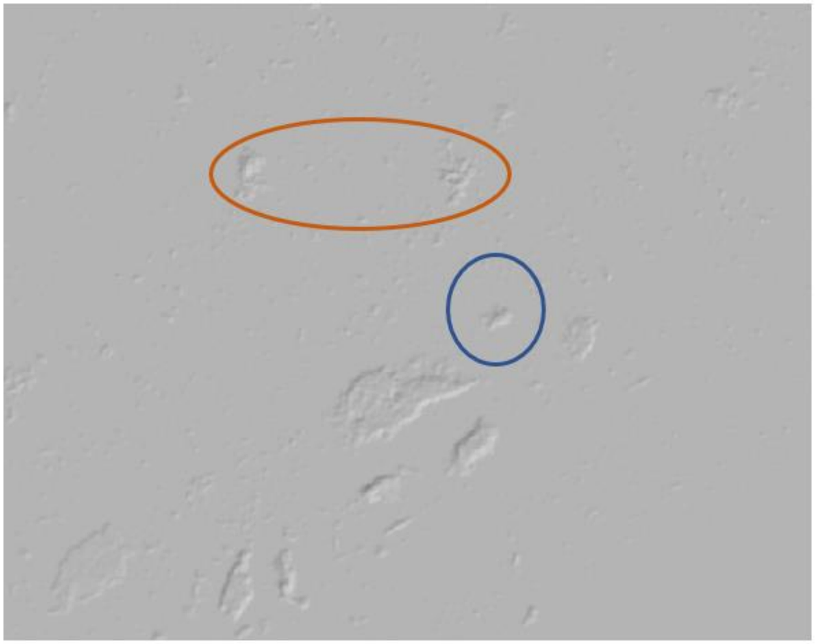

Figure 4.7 Delineated scar visible through hillshade (blue) with two non-delineated scars above (orange). Original DEM (USGS, 2017) converted in ArcGIS Pro (Esri, 2021a) and edited in PowerPoint (Microsoft, 2021b)

The NWI identified the two largest pools, as well as two mid-sized pools. Using 2010 infrared from the PASDA Imagery Navigator (see Figure 4.8), it is clear why Pools 1, 4, and 5 were identified, since they are clearly visible. It should be noted, however, that these are more recent images compared to the 1983 infrared images that were used in the NWI (USFWS, 1983). Pool 2 may have been missed, because the analyst believed Pool 1was the combination of the two, although the NWI delineation does not overlap at all with the LKIA Pool 2 delineation. Pool 3 is another clearly visible pool which was missed by the analyst, possibly because it is thinner and blends more into the nearby trees. Pool 7 was likely identified solely by its depression, since more than half of the pool is covered with grass that makes it blend in with the surrounding land. While still overlapping the respective pools, all of the NWI delineations were off center from the LKIA delineations, compared to the OBIA and the WHAT which either were fully contained by, or fully contained, the LKIA delineations.

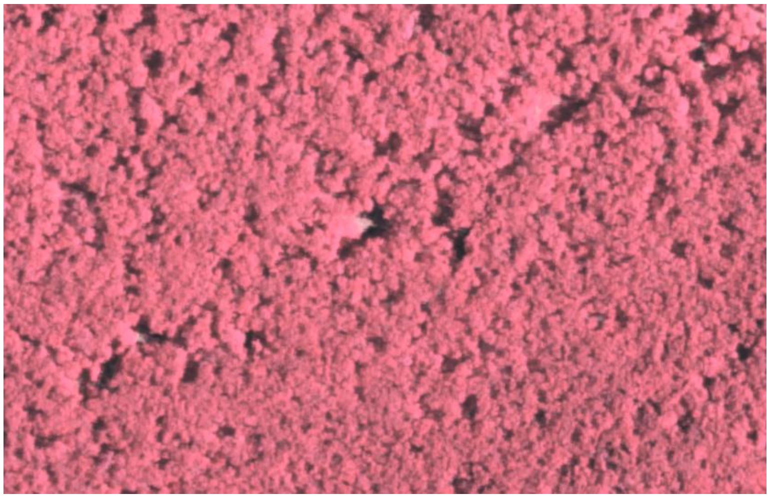

Figure 4.8 Statewide Infrared 2010 aerial display imagery of Pools 1-10 from Pennsylvania Spatial Data Access Imagery Navigator (PASDA, 2021)

The OBIA identified the first five pools, which are clearly a different color than the surrounding land when using leaf-off 2018-2020 Color imagery on PASDA (see Figure 2.4). Pool 7 could have been missed because of the covering dead grass.

The WHAT identified four pools and was the only method to delineate the solifluction Pool 11. Furthermore, it was the only method to recognize the often-saturated middle section between Pools 1 and 2. Because the LiDAR data was collected in the late fall and the pools are so shallow, there is a high probability the pools were frozen or semi-frozen (USGS, 2017). This would create a flat, hard surface that could potentially cover up the depression below it and could explain why the WHAT missed so many pools. It should also be noted that, while not able to identify more than four pools in one run, the WHAT identified smaller pools like Pool 6 and

Pool 9 in separate parameter iterations, which could theoretically make it the most successful identifier of the BJT FVAPs in this study.

4.3 Delineation Methods Morphology Measurements Comparison

Table 4.4 shows the percent error of morphology measurements for each delineation method when compared to the reference manual measurements (see Appendix C for raw measurements and calculations). When analyzing this data, it is important to note that the pools are constantly in a state of flux, especially on a seasonal scale. Therefore, you can have more reliable data sources (e.g., manual measurements and the LKIA), but it is not surprising to have variability when comparing their measurements. Even manual measurements, held to be the most accurate delineation method, can be influenced by encroaching shrubbery and weak hydrologic indicators. Therefore, high amounts of error for some of the LKIA measurements (e.g., for Pools 1 and 4) are expected. Regardless, the LKIA measurements had the least average error across all four measurements.

Table 4.4 Morphology Measurement percent error comparisons between the four methods of delineation and the manual fieldwork measurements

Percentage Comparison with **Perimeter** Manual Measurements	Pool 1	Pool 2	Pool 1+2	Pool 3	Pool 4	Pool 5	Pool 6	Pool 7	Pool 8	Pool 9	Pool 10	Pool 11	Average
Taylor Digitization	48.13	13.99	---------	30.67	4.05	11.72	7.73	0.75	7.85	16.15	1.49	14.23	14.25
NWI	23.81	---------	---------	---------	39.08	15.67	---------	20.43	---------	---------	---------	---------	24.75
OBIA	56.29	59.95	---------	42.35	23.71	7.63	---------	---------	---------	---------	---------	---------	37.99
WHAT PASDA 2017	---------	---------	50.87	---------	---------	---------	---------	33.99	---------	---------	---------	41.37	42.08
Percentage Comparison with **Surface Area** Manual Measurements	Pool 1	Pool 2	Pool 1+2	Pool 3	Pool 4	Pool 5	Pool 6	Pool 7	Pool 8	Pool 9	Pool 10	Pool 11	Average
Taylor Digitization	75.35	11.91	---------	55.02	110.85	33.43	21.18	10.01	49.17	0.95	27.23	13.99	37.19
NWI	41.68	---------	---------	---------	12.06	74.34	---------	29.81	---------	---------	---------	---------	39.47
OBIA	85.30	82.00	---------	71.38	4.89	1.30	---------	---------	---------	---------	---------	---------	48.97
WHAT PASDA 2017	---------	---------	54.59	---------	---------	---------	---------	3.10	---------	---------	---------	120.86	59.52
Percentage Comparison with **Length** Manual Measurements	Pool 1	Pool 2	Pool 1+2	Pool 3	Pool 4	Pool 5	Pool 6	Pool 7	Pool 8	Pool 9	Pool 10	Pool 11	Average
Taylor Digitization	46.74	7.11	---------	19.38	51.06	13.91	0.44	9.51	8.89	4.70	1.09	2.43	15.02
NWI	41.31	---------	---------	---------	13.65	5.59	---------	13.43	---------	---------	---------	---------	18.49
OBIA	54.16	66.03	---------	50.56	11.44	26.87	---------	---------	---------	---------	---------	---------	41.81
WHAT PASDA 2017	---------	---------	20.24	---------	---------	---------	---------	23.58	---------	---------	---------	47.52	30.45
Percentage Comparison with **Width** Manual Measurements	Pool 1	Pool 2	Pool 1+2	Pool 3	Pool 4	Pool 5	Pool 6	Pool 7	Pool 8	Pool 9	Pool 10	Pool 11	Average
Taylor Digitization	47.83	1.74	---------	27.25	53.21	23.76	15.78	6.00	45.56	12.55	45.40	22.35	27.40
NWI	11.72	---------	---------	---------	16.06	99.15	---------	1.89	---------	---------	---------	---------	32.21
OBIA	62.25	46.14	---------	44.30	23.78	48.97	---------	---------	---------	---------	---------	---------	45.09
WHAT PASDA 2017	---------	---------	65.24	---------	---------	---------	---------	12.25	---------	---------	---------	61.96	46.48
Pool 1+2 is considering Pools 1, 2 and the section between them as a single pool													

The clear frontrunner of the remaining delineation methods was the NWI. In all but the perimeter measurements, the NWI had only an additional 3-5 percent error compared to the LKIA. Although higher, the perimeter error was only about ten percent higher than the LKIA. Next came the OBIA, having an error roughly between 40-50 percent and between 10-20 percent higher than the LKIA. The OBIA was followed closely behind by the WHAT. The WHAT had a much greater range from 30-60 percent. Only in Length was the WHAT considered more accurate than the OBIA. For Length, the WHAT was roughly fifteen percent higher than the LKIA. For the rest of the measurements, the WHAT was closer to 20-30 percent higher than the LKIA. Surface error produced the highest error for all the measurements.

While the NWI was split between overestimating and underestimating measurements, the OBIA tended to underestimate measurements and the WHAT tended to overestimate measurements (see Appendix C). It is unknown whether changing the WHAT parameters can reduce measurement error while still identifying the same pools, but there is that potential. Perimeter will likely always have a large amount of error, due to the roughness of the delineations. The WHAT has far more folds and edges than any of the other methods, including manual delineations, which tend to have smooth and straight edges. Although this may appear as more inaccurate when compared to other delineations, in reality it could present a far more realistic representation of the boundary between a FAVP and upland (see Figure 4.9).

Figure 4.9 Forested Appalachian Vernal Pools often have rough and folding boundary lines with uplands. Image from (Blackman, 2020)

From a qualitative aspect, the shape of the WHAT delineations are far more accurate than any of the other methods' delineations, including the LKIA. While the LKIA has two ovals for Pools 1 and 2, not to mention the large off-center NWI Pool 1, the WHAT delineated the arc shape that is often formed when the pools are connected (see Figure 4.10). The arc also has the narrowing neck where the middle section moves from the wider Pool 1 to the narrower Pool 2. Pool 7 is similarly accurate, with the narrow northeast end of the pool, where the grass does not cover the surface. While the LKIA has this shape, the NWI does not. Pool 11 is similarly qualitatively accurate.

Figure 4.10 Pools 1 and 2 are often connected in saturated conditions. Image from (Blackman, 2020)

The Laurel Run small reservoir, while not a FAVP, was included in the delineations of the WHAT, the OBIA, and the NWI in order to demonstrate the WHAT's potential. Designed for larger depressions, the WHAT delineation perfectly outlines the reservoir, while the OBIA and the NWI delineations do not fully contain it (see Figure 4.11).

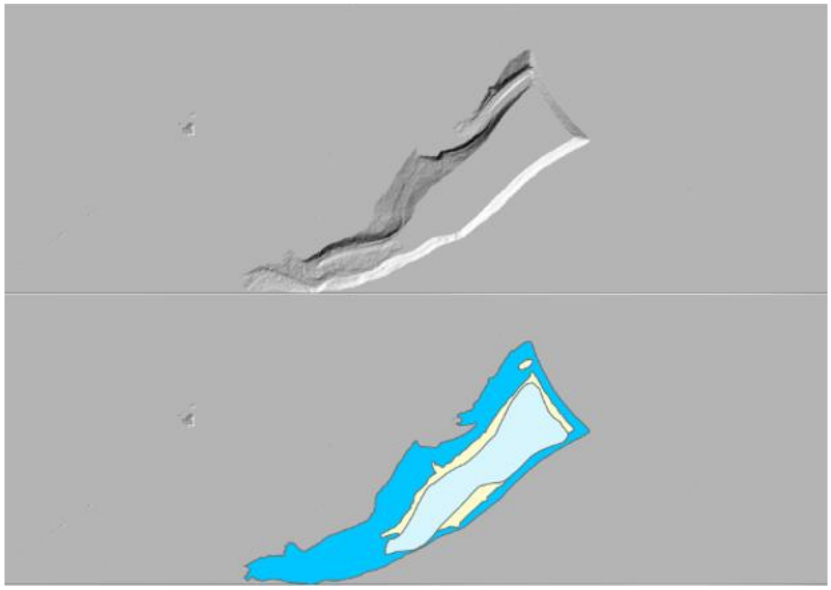

Figure 4.11 Laurel Run Reservoir comparison between hillshade (top) and delineations of WHAT (turquoise), OBIA (tan), and NWI (light blue). Original DEM (USGS, 2017) viewed in ArcGIS Pro (Esri, 2021)

4.4 Regional Inventory Potential

It has been established that the NWI is a fairly accurate method for FVAP delineations. However, this method still suffers from being time and labor intensive. The question therefore remains: are either of the two automated modeling methods (OBIA or the WHAT) adequate enough to be used for an updated regional inventory of FAVPs? As it stands, this thesis suggests that the OBIA would be better suited to producing this inventory, both because of its better identification success and because of its slightly more accurate morphology measurements.

However, the WHAT produces results that have the more accurate shape and perimeter edge, the ability to recognize solifluction pools, and the ability to identify different pools with different parameters, giving it the potential to produce better results with more research on the influence of its parameters.

Chapter 5

Conclusion

This thesis supports the accuracy of the NWI for delineating proper morphology measurements of FAVPs, but finds that qualitative shape and position are not as accurate. This thesis also finds that of the two less-accurate automated delineation modeling methods, the OBIA and the WHAT, the OBIA would currently be best suited to creating a regional inventory of FAVPs. However, it is acknowledged that the WHAT has some potential to improve its data quality by changing the input parameters, since this thesis largely views it as a black box.

Considering its original intended use in delineating large prairie potholes, the WHAT had marked success in recognizing and delineating FAVPs, even if their measurements were not very accurate. It has been shown that changing parameters affects the delineation results of the FAVPs. Since this toolbox is fully open-source and the Python scripts are available, a coding background could be used to better understand how the tools function, which parameter values may be best, and whether code could be revised to better suit the region. Furthermore, the code can be translated into Python 3, making this toolbox adaptable.

This paper indicates the number of different delineation methods that exist and are being developed to improve the knowledge base of crucial vernal pool ecosystems. Equally important, this thesis highlights the sheer amount of open-source data and software that is available for this subject area. This means that with a reliable delineation method, governmental agencies, non-profits, non-governmental organizations, and the private sector can all utilize the benefits of FAVP delineations, regardless of financial standing. This would have a major impact on both conservation and mitigation efforts to preserve FAVPs.

Appendix A

Extract Sink Parameter Tests Shapefile Outputs

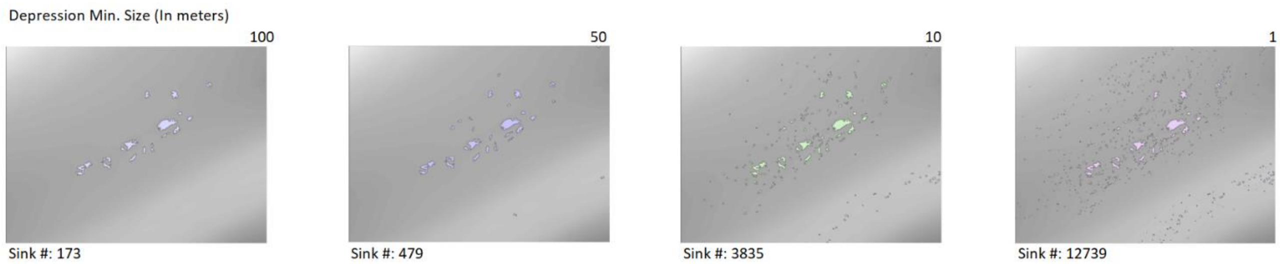

Figure A.1 BJT shapefile outputs from various Depression Minimum Size (meters) parameter values for Extract Sink tool testing. Corresponding sink numbers are for the BJT larger area. DEM (PADCNR, 2006-2008) viewed in ArcMap (Esri, 2021b) and edited in Excel (Microsoft, 2021a)

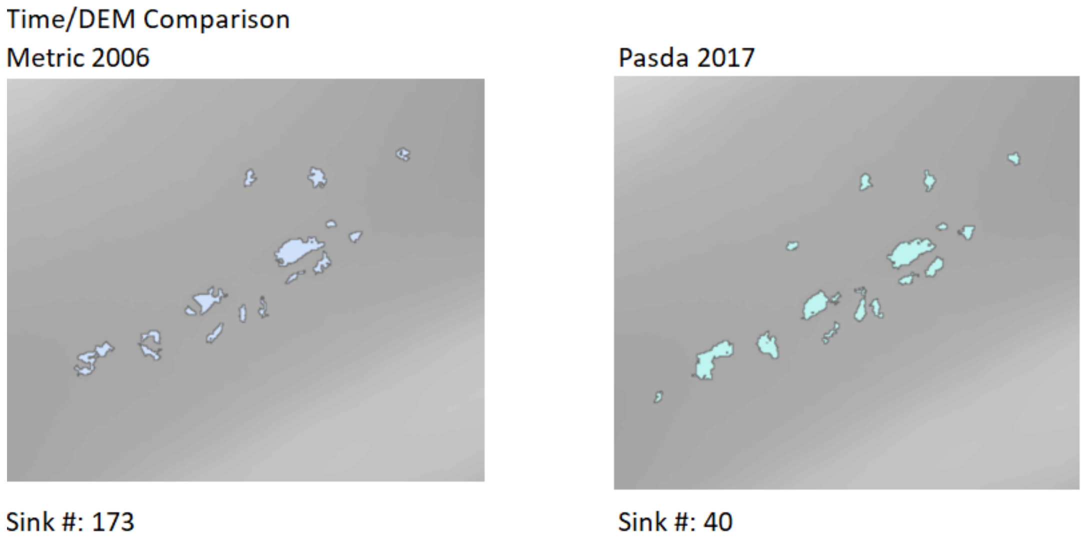

Figure A.2 BJT shapefile outputs from various DEM Raster parameter inputs for Extract Sink tool testing. Corresponding sink numbers are for the BJT larger area. DEM (PADCNR, 2006-2008) viewed in ArcMap (Esri, 2021b) and edited in Excel (Microsoft, 2021a)

Appendix B

Identify Depressions Parameter Tests Shapefile Outputs

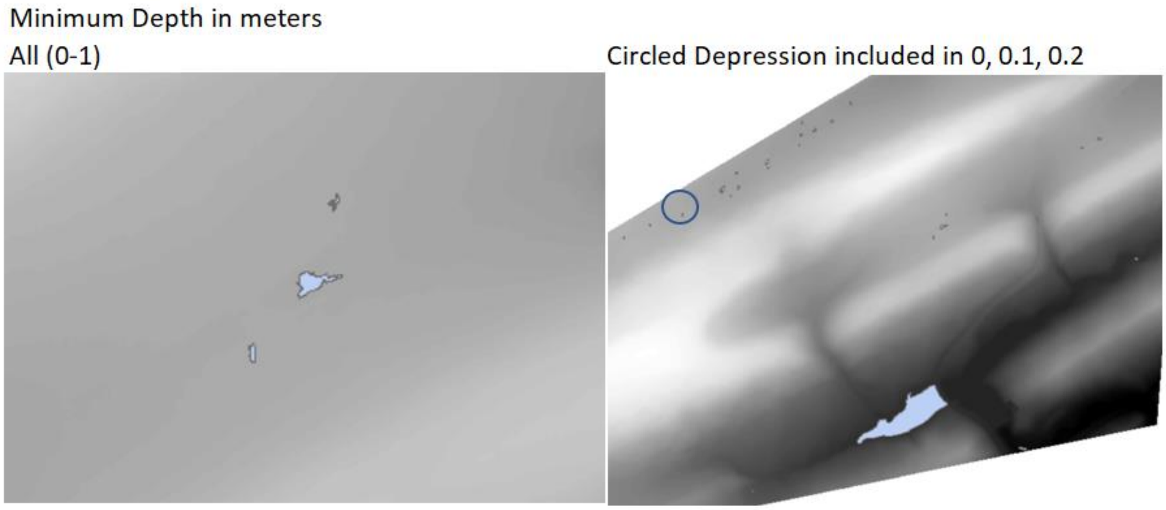

Figure B.1 BJT (left) and larger area (right) shapefile outputs from various Minimum Depth (meters) parameter values for Identify Depressions tool testing. DEM (PADCNR, 2006-2008) viewed in ArcMap (Esri, 2021b) and edited in Excel (Microsoft, 2021a)

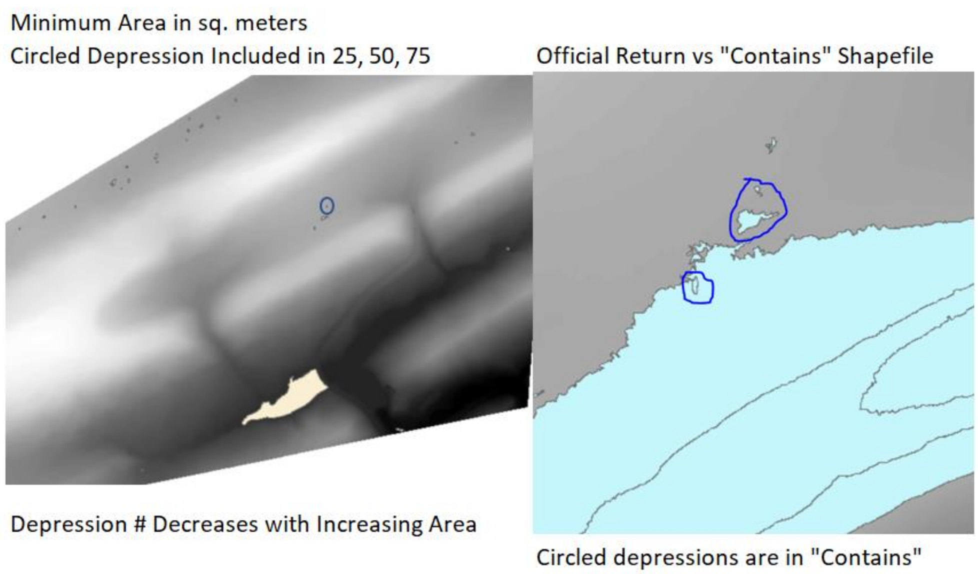

Figure B.2 BJT larger area shapefile output from various Minimum Area (sq. meters) parameter values for Identify Depressions tool testing (left). Comparison of the Official shapefile return to the Contains shapefile return (right). DEM (PADCNR, 2006-2008) viewed in ArcMap (Esri, 2021b) and edited in Excel (Microsoft, 2021a)

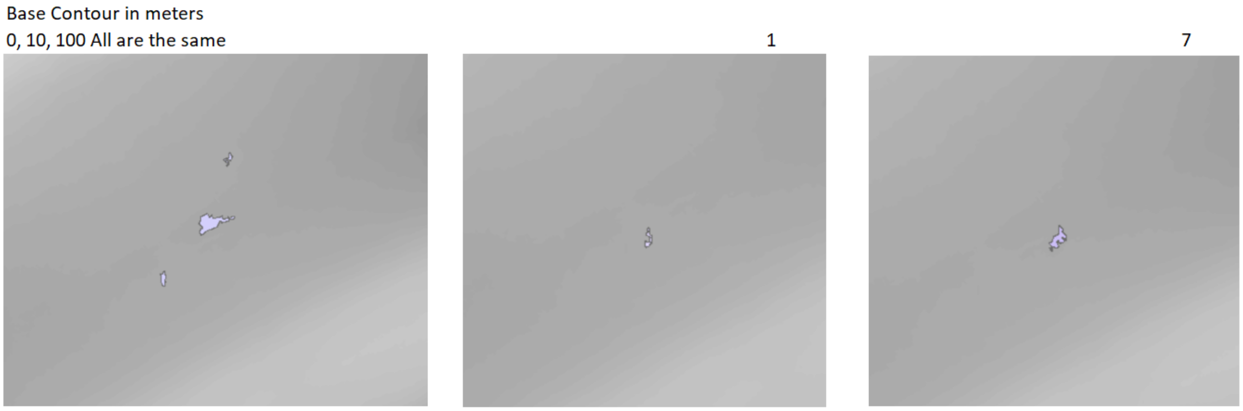

Figure B.3 BJT shapefile outputs from various Base Contour (meters) parameter values for Identify Depressions tool testing. DEM (PADCNR, 2006-2008) viewed in ArcMap (Esri, 2021b) and edited in Excel (Microsoft, 2021a)

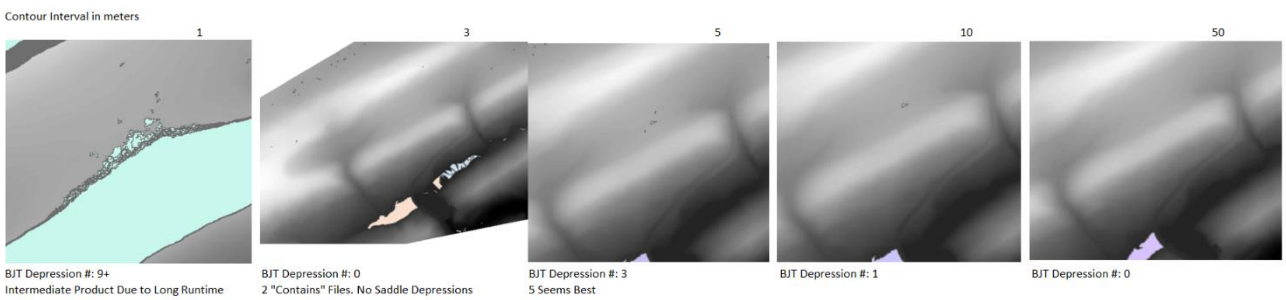

Figure B.4 BJT larger area shapefile outputs from various Contour Interval (meters) parameter values for Identify Depressions tool testing. DEM (PADCNR, 2006-2008) viewed in ArcMap (Esri, 2021b) and edited in Excel (Microsoft, 2021a)

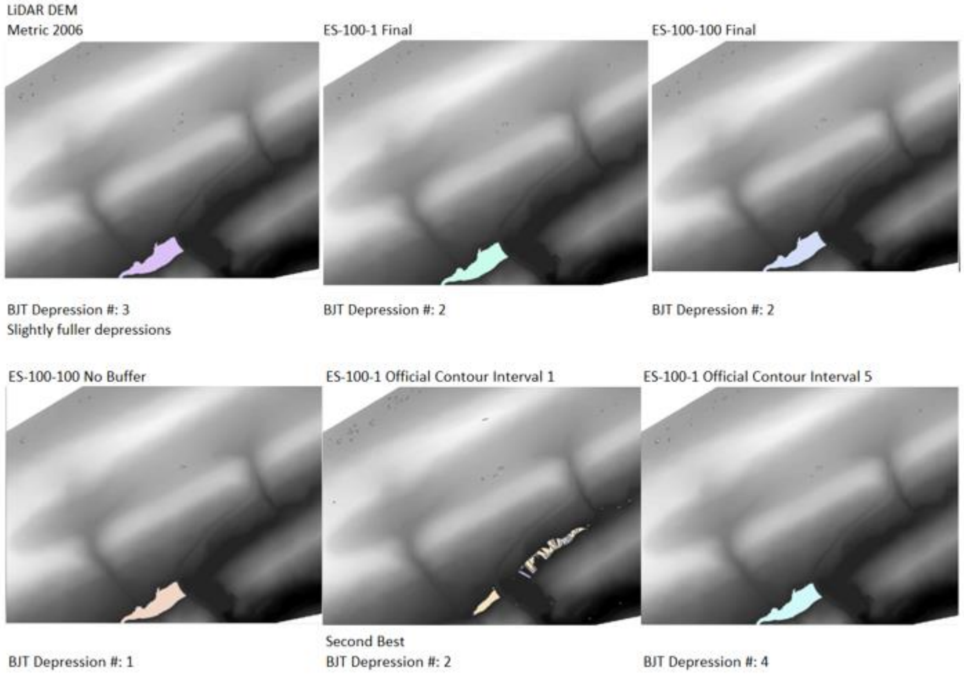

Figure B.5 BJT larger area shapefile outputs from various LiDAR DEM parameter inputs for Identify Depressions tool testing. DEM (PADCNR, 2006-2008) viewed in ArcMap (Esri, 2021b) and edited in Excel (Microsoft, 2021a)

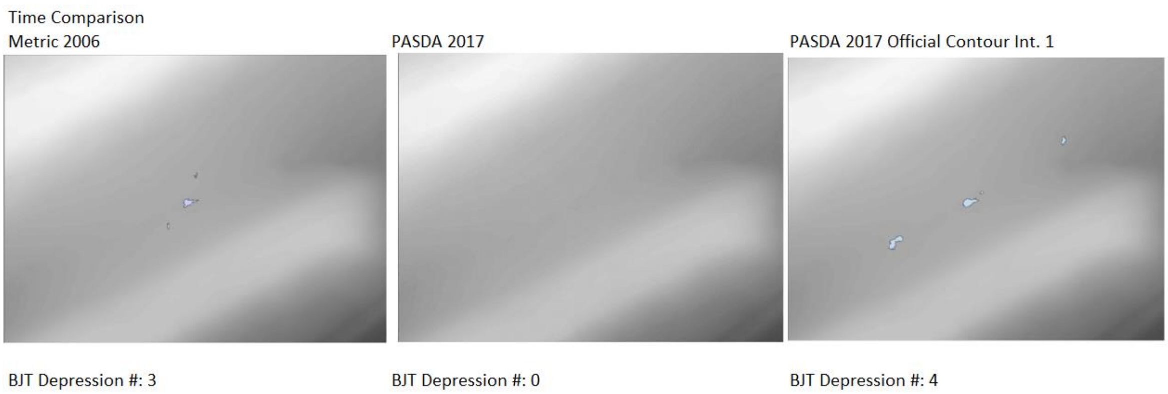

Figure B.6 BJT shapefile outputs from Time Comparison Identify Depressions tool testing. DEM (PADCNR, 2006-2008) viewed in ArcMap (Esri, 2021b) and edited in Excel (Microsoft, 2021a)

Appendix C

Raw Data from Morphology Measurement Comparison Test

Table C.1 Perimeter raw delineation measurements. All values are in meters. Pool 1-2 is the often saturated section between Pools 1 and 2. Pool 1+2 is considering Pools 1, 2, and 1-2 as a single pool

	Manual	LKIA	NWI	OBIA	WHAT
Pool 1	88.73	46.03	109.86	38.78	---------
Pool 2	63.79	54.87	---------	25.55	---------
Pool 1-2	19.72	---------	--------	---------	---------
Pool 1+2	158.16	---------	---------	---------	238.61
Pool 3	92.17	63.90	---------	53.14	---------
Pool 4	134.14	128.71	81.72	102.34	---------
Pool 5	71.00	79.32	82.12	65.59	---------
Pool 6	33.01	30.46	---------	---------	---------
Pool 7	143.47	142.39	114.15	---------	192.23
Pool 8	29.60	27.28	---------	---------	---------
Pool 9	62.54	52.44	---------	---------	---------
Pool 10	60.81	59.91	---------	---------	---------
Pool 11	64.80	55.58	---------	---------	91.61

Table C.2 Surface Area raw delineation measurements and calculations. All values are in sq. meters. Pool 1-2 is the often saturated section between Pools 1 and 2. Pool 1+2 is considering Pools 1, 2, and 1-2 as a single pool. For solely Surface Area, Pool 1+2 will be based on the sum of the surface areas of the individual pools/the section between them, because the shape of the combined two pools does not resemble an oval

	Manual	LKIA	NWI	OBIA	WHAT
Pool 1	624.91	154.02	885.37	91.84	----------
Pool 2	240.52	211.87	---------	43.30	----------
Pool 1-2	28.27	----------	---------	---------	----------
Pool 1+2	893.70	----------	---------	---------	1381.61
Pool 3	515.38	231.83	---------	147.51	----------
Pool 4	515.38	1086.69	453.23	540.56	----------
Pool 5	272.92	364.15	475.81	276.46	----------
Pool 6	67.86	53.49	---------	---------	----------
Pool 7	1165.53	1048.86	818.08	---------	1201.61
Pool 8	33.08	49.35	---------	---------	----------
Pool 9	165.48	167.05	---------	---------	----------
Pool 10	198.91	253.07	---------	---------	----------
Pool 11	174.64	199.07	---------	---------	385.72

Table C.3 Length raw delineation measurements. All values are in meters. Pool 1-2 is the often saturated section between Pools 1 and 2. Pool 1+2 is considering Pools 1, 2, and 1-2 as a single pool

	Manual	LKIA	NWI	OBIA	WHAT
Pool 1	29.8	15.87	42.1	13.66	--------
Pool 2	23.2	21.55	-------	7.88	--------
Pool 1-2	7.5	--------	-------	-------	--------
Pool 1+2	57.7	--------	-------	-------	69.38
Pool 3	34.0	27.41	-------	16.81	--------
Pool 4	34.0	51.36	29.4	37.89	--------
Pool 5	29.7	33.83	31.4	21.72	--------
Pool 6	13.5	13.44	-------	-------	--------
Pool 7	53.0	58.04	45.9	-------	65.50
Pool 8	11.7	10.66	-------	-------	--------
Pool 9	21.5	22.51	-------	-------	--------
Pool 10	20.1	19.88	-------	-------	--------
Pool 11	21.8	22.33	-------	-------	32.16

Table C.4 Width raw delineation measurements. All values are in meters. Pool 1-2 is the often saturated section between Pools 1 and 2. Pool 1+2 is considering Pools 1, 2, and 1-2 as a single pool

In Meters	Manual	LKIA	NWI	OBIA	WHAT
Pool 1	26.7	13.93	29.8	10.08	----------
Pool 2	13.2	12.97	-------	7.11	----------
Pool 1-2	4.8	--------	-------	-------	----------
Pool 1+2	14.5	--------	-------	-------	23.96
Pool 3	19.3	14.04	-------	10.75	----------
Pool 4	19.3	29.57	22.40	23.89	----------
Pool 5	11.7	14.48	23.30	17.43	----------
Pool 6	6.4	5.39	-------	-------	----------
Pool 7	28.0	26.32	27.5	-------	31.43
Pool 8	3.6	5.24	-------	-------	----------
Pool 9	9.8	11.03	-------	-------	----------
Pool 10	12.6	18.32	-------	-------	----------
Pool 11	10.2	12.48	-------	-------	16.52

Appendix D

Tutorial: Importing LiDAR Data from PASDA and Creating DEMs

1. Go to pasda.psu.edu
2. On pasda.psu.edu, click the tab at the top named “Apps and Tools”
3. Select the “Pennsylvania Imagery Navigator”
4. You will now see an interactive map of Pennsylvania that you can zoom in on by double clicking (not right clicking). You can also zoom by scrolling, but this method is more sensitive. On this interactive map, zoom or pan to whatever area you are interested in and right click the area
5. A “PASDA Download Links” box appears. Within this box, click the tab labeled “Lidar, Topo”
6. The different tiles are listed by row with their attributes listed in columns (Extent, Source, Metadata, LAS data, etc.). Click the hyperlinks in the “Show Tile Extent” for a highlighted box to appear on the map showing the extent of each tile. Use this to choose the tile that will work best for you. This tutorial will be using the “21001990PAN” tile
7. The easiest way to obtain the LAS data is to click the “download” hyperlink under the “LAS” column. Should this successfully download the .zip file proceed to step 15. Sometimes, however, the download link does not respond and you will need to access the data another way
8. Open another tab and go to pasda.psu.edu again
9. Under “Data Shortcuts” click “Lidar and Elevation”
10. Scroll Down and click “PAMAP Program – LiDAR LAS files”

11. Select “Download”. You will now be taken to a directory with file path: /pub/pasda/pamap/pamap_lidar/cycle1
12. Select the directory “LAS/”. Your file path is now: /pub/pasda/pamap/pamap_lidar/cycle1/LAS/
13. To determine the rest of the file path, switch to the other tab of the interactive map and the “PASDA Download Links” box and hover your cursor over the “download” link in the specific row of the “LAS” column
14. Somewhere on your screen (most likely the bottom left corner), a gray textbox will appear with the full path of the downloadable LAS file. This is the same path that can be used on the directory tab to find the file. Switch tabs and navigate to it
15. Once you have downloaded the .zip file, find it in your “Downloads” folder (assuming you have a Windows computer)
16. Right click the .zip file and “Extract All” it to whatever location you choose
17. Start up ArcGIS Pro (Esri, 2021a)
18. Create a new project with a blank “Map” template
19. On the “Insert” ribbon tab in the “Project” group, use the “Add Folder” button to add the folder connection
20. In the “Catalog” pane, expand “Folders” to see your added folder
21. Right click the .las file and “Add To Current Map”
22. In the “Geoprocessing” pane, search for “LAS to raster”
23. Select the “LAS Dataset to Raster” tool (Esri, n.d.-e)

24. The “LAS Dataset to Raster” tool opens up within the pane

    Input LAS Dataset: The .las file

    Output Raster: The name and location of the new raster file type

    Change other parameters as you would like (the default was used for this tutorial). This will create the DEM on the map

25. If you had to download multiple LAS tiles from pasda.psu.edu, repeat steps 19-24 until you have created all of your DEMs

26. Instead of creating a DEM from the raw LAS data, you may wish to use the DEM files that are available on pasda.psu.edu. The process is the same as steps 1-16, but use the “download” link under the “DEM” column instead of the “LAS” column. One pro of downloading the DEM files directly is that they are free of flight-line “scars” (see Figure D.1) that can be present when using the raw LAS data. This would not be ideal for flow routing. One con of downloading the DEM directly is that the extent of the DEM can sometimes be smaller than the extent you could have by using the raw LAS data

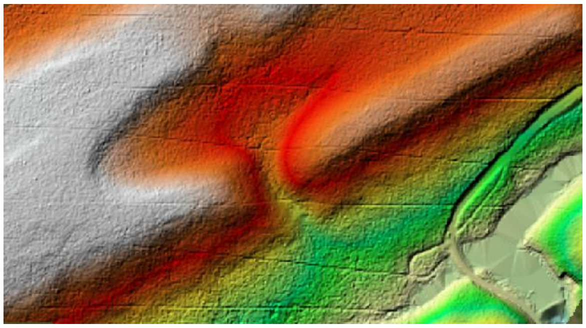

Figure D.1 Flight-line scars on a DEM when created from raw LiDAR data. Data was sourced from PASDA (USGS, 2017) and converted to a DEM in ArcGIS Pro (Esri, 2021a)

Appendix E

Tutorial: Geoprocessing DEMs (Projecting, Merging, Clipping, & Altering Resolution)

1. Spatial information utilizes a coordinate system that depicts the relative location and size of the layers on a map. Having layers with different coordinate systems (also known as projections) on a map can create error. Although ArcGIS Pro will project on the fly (temporarily change the projections of all layers to the projection of the first added layer) when viewing your map, the projections need to manually be made uniform in order to perform alterations or analysis (Smith, 2020). The "Project Raster" tool can be used to do this for DEMs and other rasters (Esri, n.d.-g).
2. Add all of the relevant layers (in this case DEMs) to your current map
3. In the "Geoprocessing" pane, search for "Project Raster"
4. Select the "Project Raster" tool

5. The “Project Raster” tool opens up within the pane (Esri, n.d.-g)

   Input Raster: The raster you wish to project onto a new coordinate system

   Output Raster Dataset: The name, location, and file type (e.g., .tif) (leave out the file type ending if you want it stored in a geodatabase)

   Output Coordinate System: Select the coordinate system of any layer currently added to the map by choosing that layer (recommended). You can also choose a different coordinate system or create a new coordinate system

   Geographic Transformation: The function used to transform the spatial data. This will automatically populate once you select an output coordinate system

   Resampling Technique: The statistical method to resample the DEM. “Nearest” and “Majority” are generally only used for discrete data. DEMs are continuous data, so you can also choose between: “Bilinear” (Less intensive/precise) and “Cubic” (More intensive/precise)

   Output Cell Size: You can select the cell size (resolution) of any layer currently added to the map by choosing that layer, or you can specify the cell size yourself in the “X” and “Y” fields

   Registration Point: Optional specification of an anchor point

   This will project the selected DEM onto a new coordinate system with a new resolution

6. If you have multiple raster layers (in this case DEMs) that you need to combine to create a single, larger layer, you can use the “Mosaic to New Raster” geoprocessing tool (Esri, n.d.-f)
7. Add each of the individual DEMs to a current map (new or existing) in ArcGIS Pro (Esri, 2021a)

8. Once all of the relevant DEMs are added, open the "Geoprocessing" pane and search for "Mosaic to New Raster"
9. Select the "Mosaic to New Raster" tool that is a part of "Data Management Tools"
10. The "Mosaic to New Raster" tool opens up within the pane (Esri, n.d.-f)

    Input Rasters: Next to "Input Rasters" is a dropdown arrow which can be used to select the relevant DEMs that exist on the current map

    Output Location: The location of the new raster file

    Raster Dataset Name with Extension: The name and file type of the new raster file (if you are storing the file in a geodatabase, leave the file type blank)

    Spatial Reference for Raster: The coordinate system to be used for the new file (existing raster layers on the map can be used as templates)

    Pixel Type: Determines pixel resolution. Should match the pixel types of the existing rasters

    Cellsize: Should you want to limit the number of cells in the new layer

    Number of Bands: Should match the number of bands of existing rasters

    Mosaic Operator: How overlapping areas should be dealt with. Default is "Last"

    Mosaic Colormap Mode: How color scheme should be chosen for a color map. Default is "First"

    This will create the single, large DEM composed of all the individual DEMs
11. A DEM can sometimes cover a larger region than necessary. To save on processing time, the area of interest (AOI) can be clipped from the original DEM via the "Clip Raster" geoprocessing tool (Esri, n.d.-a)
12. Make sure the relevant DEM is added to the current map

13. To manually select the desired area of the DEM, you will first need to create a polygon feature of that area (Esri, n.d.-b)
14. On the "Catalog" pane, expand "Databases" and right-click the database you want to save the polygon feature in
15. Hover over "New" and select "Feature Class", which will open the "Create Feature Class" pane
16. Create a file path name under "Name" (cannot have spaces) and optionally create a more user-friendly name under "Alias" (can have spaces)
17. Settings can all be left as default, but make sure on "Page 3/6" that the spatial reference is the same as your DEM/Map
18. Click "Finish". The polygon feature is created in the specified database and should be added to your current map
19. In the "Edit" tab, in the "Features" group, click "Create"
20. The "Create Features" pane pops up, with your feature class listed under "Templates"
21. Click the feature class and select whichever drawing option you would like
22. After your drawing option is selected, draw out the polygon on your current map. Click to place vertices and move the mouse to draw out the line. Double click to finish the polygon. You are now ready to clip

    Note: Because the map is drawn by on the fly projection, the basemap layer projection can remain as "WGS 1984 Web Mercator (auxiliary sphere)" as long as the DEM, polygon feature class, and the current map all have the same projection. You can use the "Imagery" basemap and lower the transparency of the DEM layer to help with recognizing your desired area (Smith, 2020)

23. In the “Geoprocessing” pane, search for “Clip Raster”
24. Select the “Clip Raster” tool
25. The “Clip Raster” tool opens up within the pane (Esri, n.d.-a)

    Input Raster: The DEM that you wish to clip

    Output Extent: Select the created polygon (the area you want)

    Rectangle: The coordinates should automatically update

    Use Input Features for Clipping Geometry: Select this so that DEM will clip exactly to the polygon. Option appears once **Input Raster** selected

    Output Raster Dataset: The name, location, and file type (e.g., .tif) (leave out the file type ending if you want it stored in a geodatabase)

    NoData Value: Can be left as default

    Maintain Clipping Extent: Leave unchecked. Otherwise, the alignment of cells will be altered so that the clipped DEM has the same number of cells as the polygon

    This will clip the single, large DEM to the desired shape/size
26. Changing the resolution of a DEM can help make viewing data clearer. Higher resolutions can show more distinction between points, while lower resolutions can help cancel noise. A DEM can be reproduced with a different resolution with the “Resample” tool (Esri, n.d.-i)
27. In the “Geoprocessing” pane, search for “Resample”
28. Select the “Resample” tool

29. The “Resample” tool opens up within the pane (Esri, n.d.-i)

Input Raster: The DEM to be copied

Output Raster Dataset: The name, location, and file type (e.g., .tif) (leave out the file type ending if you want it stored in a geodatabase)

Output Cell Size: Can be left blank

X & Y: This will be where you determine the resolution. Typing 5 in each will create a resolution of 5 units by 5 units (e.g., 5m x 5m)

Resampling Technique: The statistical method to resample the DEM. “Nearest” and “Majority” are generally only used for discrete data. DEMs are continuous data, so you can also choose between: “Bilinear” (Less intensive/precise) and “Cubic” (More intensive/precise)

This will create a separate DEM of the same area but a different resolution

Appendix F

Tutorial: Geoprocessing DEMs (Filling and Breaching)

1. DEMs normally have individual cells or groups of cells that incorrectly have a lower elevation than their surrounding neighboring cells. These spurious depressions (also known as artifacts) occur due to error during the data collection process. These artifacts can trap modeled flow, so it is useful to alter them. One method is filling, where the cell(s) have its/their elevation raised to the lowest neighboring cell. This allows flow to continue on its way. There are many different filling techniques. This tutorial will first use the “Fill Depressions" tool as part of the WhiteboxTools-ArcGIS toolset (Lindsay, 2016) and then the “Fill” tool as part of the ArcGIS Pro toolset (Esri, n.d.-c; Esri, 2021a). The “Fill Depressions” tool is a modified version of the Wang & Liu (2006) filling algorithm (Lindsay, 2021) and the “Fill” tool is a version of the Planchon & Darboux (2002) filling algorithm
2. First you will need to install the WhiteboxTools-ArcGIS toolbox (Lindsay, 2016)
3. Follow the instructions under the “Installation” section on the GitHub page: https://github.com/giswqs/WhiteboxTools-ArcGIS#license
4. Once the toolbox is added to ArcGIS Pro (Esri, 2021a), go to the relevant Current Map with your existing DEM
5. Per the WhiteboxTools User Manual, the “Fill Depressions” tool does not fill NoData cells, so these cells will need to be filled first (Lindsay, 2021)
6. Both the “Clip Raster” and the “Copy Raster” ArcGIS Pro tools have a default setting of labeling cells with a value of 3.4E+38 as “NoData”. If you haven’t used those tools, you

can use the “Set NoData Value” tool (not included in this Appendix) to set the value for NoData cells (Lindsay, 2021)

7. To check whether NoData cells exist, use the WhiteboxTools “Is No Data” tool (Lindsay, 2021)
8. In the “Geoprocessing” pane, search for “Is No Data”
9. Select the “Is No Data” tool
10. The “Is No Data” tool opens up within the pane (Lindsay, 2021)

    Input File: The DEM you wish to check

    Output File: The name, location, and file type of resultant raster

    The Output raster will label NoData cells as “1” and other cells as “0”. In a black and white color scheme, the raster will therefore show NoData cells as white and regular cells as black.

11. Once you have visualized the NoData in your DEM, you can move on to filling the NoData cells with the WhiteboxTools “Fill Missing Data” (Lindsay, 2021)
12. In the “Geoprocessing” pane, search for “Fill Missing Data”
13. Select the “Fill Missing Data” tool

14. The “Fill Missing Data” tool opens up within the pane (Lindsay, 2021)

    Input File: The DEM you wish to fill the NoData cells

    Output File: The name, location, and file type of the resulting NoData filled raster

    Filter Dimension: Maximum size a NoData group of cells can be before not filled

    IDW Weight (Exponent) Value: The larger the IDW Weight, the more the filled elevation is determined by nearby cell values than further surrounding cell values (Esri, n.d.-d)

    Exclude edge-of-raster-connected NoData cells?: If selected, will ignore the No-Data values along the edge of the raster. This is useful for clipped DEMs, which leave NoData values for the cells that were clipped off. In that case, you wouldn’t want those cells refilled

    The DEM will now have all desired NoData cells filled to statistically estimated levels

15. With all the desired NoData cells filled, you are now ready to use the “Fill Depressions” tool
16. In the “Geoprocessing” pane, search for “Fill Depressions”
17. Select the “Fill Depressions” tool

18. The “Fill Depressions” tool opens up within the pane (Lindsay, 2021)

    Input DEM File: The DEM you wish to fill

    Output File: The name, location, and file type of the resulting filled raster

    Fix Flat Areas?: Selecting this will remove flat areas that can cause problems for flow routing. They are fixed by the creation of a slight gradient, starting from the outlet of the flat area and based on the topography of the input DEM

    Flat Increment Value (Z Units): Optional way to choose the elevation increments for fixing the flat gradient. Recommended to use default settings and leave this blank

    Maximum Depth (Z Units): Optional maximum depth allowed for a depression to be filled. Not placing a value here could potentially cause the tool to fill up a large portion of the DEM to the same value, so it is recommended you do so

    The DEM will now have its depressions filled and flat areas removed. The number of remaining depressions depends on what was entered for the optional field “Maximum Depth (Z Units)”

19. To fill a DEM solely using ArcGIS Pro (Esri, 2021a), you can use the “Fill” tool.
20. On the relevant Current Map, open up the “Geoprocessing” pane
21. In the “Geoprocessing” pane, search for “Fill”
22. Select the “Fill (Spatial Analyst Tools)” tool

23. The “Fill” tool opens up within the pane (Esri, n.d.-c)

    Input Surface Raster: The DEM you wish to fill

    Output Surface Raster: The name, location, and file type of the resulting filled raster (leave out the file type ending if you want it stored in a geodatabase)

    Z Limit: Optional maximum allowed difference between the bottom of the depression and the nearest pour point. Any depression larger than the “Z limit” value will not be filled. If left empty, all depressions will be filled

    The DEM will now have its depressions filled. The number of remaining depressions depends on what was entered for the optional field “Z Limit”

24. An alternative method to filling is a process calling breaching. Much like filling, there are many different forms of breaching. The WhiteboxTools User Manual states that its “Breach Depressions Least Cost” tool was influenced by the Lindsay & Dhun (2015) breaching algorithm. Instead of filling an entire depression, “Breach Depressions Least Cost” will lower the cells between the bottom of the depression and a nearby, lower neighboring cell, essentially creating an outlet to that cell. Which neighboring cell is chosen depends on a cost efficiency calculation (changing the least amount of cell elevation). Any remaining depressions can optionally be filled. Depressions that are filled will be raised to an outlet point and then will be incrementally raised away from the outlet (in order to form a gradient towards the outlet) (Lindsay, 2021)
25. On the relevant Current Map, open up the “Geoprocessing” pane
26. In the “Geoprocessing” pane, search for “Breach Depressions Least Cost”
27. Select the “Breach Depressions Least Cost” tool

28. The “Breach Depressions Least Cost” tool opens up within the pane (Lindsay, 2021)

Input DEM File: The DEM you wish to breach/fill

Output File: The name, location, and file type of the resulting filled raster

Maximum Search Distance (Cells): The maximum radius of the area to be searched for placement of the least cost breach channel. A larger distance is more likely to find the most efficient breach channel, but is also more time intensive. For large file size DEMs this can be problematic (Lindsay & Dhun, 2015)

Maximum Breach Cost (Z Units): Optional maximum amount of elevation change (cost) allowed. Any depressions that would require a larger amount of cost will not be breached

Minimize Breach Distances?: If selected, the algorithm will use an equation that attempts to minimize both cost and distance. If not selected, the algorithm will use an equation that will solely minimize cost. This may reduce more of the cost at the expense of a greater breach distance (Lindsay, 2021)

Flat Increment Value (Z Units): Optional way to choose the elevation increments for fixing flat gradients. Recommended to use default settings and leave this blank

Fill Unbreached Depressions?: This will fill any depressions not resolved by breaching using the method discussed in the previous steps

The DEM will now have its depressions breached/filled. The number of remaining depressions depends on what was entered for “Max. Search Distance”, “Max. Breach Cost”, and “Fill Unbreached Depressions?”

BIBLIOGRAPHY

Addink, E. (2010). *Object-based image analysis*. GIM International. Retrieved October 31, 2021, from https://www.gim-international.com/content/article/object-based-image-analysis

Blackman, T. (2019). *Vernal pool mapping and geomorphology in the Appalachian Mountains of Pennsylvania* (Master's thesis, Virginia Polytechnic Institute and State University). Retrieved from https://vtechworks.lib.vt.edu/bitstream/handle/10919/89930/Blackman_TN_T_2019.pdf?sequence=1&isAllowed=y

Blackman, T. (2020). Personal drone imagery of the Ben Jacobs Trail research site

Brown, L. J. & Jung, R. E. (2005). *An introduction to Mid-Atlantic seasonal pools*. Environmental Protection Agency, Mid-Atlantic Integrated Assessment, Ft. Meade, Maryland

Bureau of Waterways Engineering and Wetlands (BWEW). (2021). *Chapter 105 water obstructions and encroachment general permit registration*. Pennsylvania Department of Environmental Protection

Clark, G. M., Behling, R. E., Braun, D. D., Ciolkosz, E. J., Kite, J. S., Marsh, B. (1993). *Central Appalachian periglacial geomorphology* (Ser. 120). The Pennsylvania State University

Colburn, E. A. (2004). *Vernal pools: Natural history and conservation.* The McDonald & Woodward Publishing Company, Blacksburg, VA

Commonwealth of Pennsylvania (CoP). (2021). Chapter 105: Dam safety and waterway management. In *Pennsylvania Code*

DiBiase, R., Greg, M., Vecchio, J. D. (2017). Stop 2: Tussey Mountain boulder fields. In (Anthony, R., Ed.) *Recent Geologic Studies and Initiatives in Central Pennsylvania* (pp. 9-11). The Pennsylvania State University & Pennsylvania Department of Conservation and Natural Resources Bureau of Topographic and Geologic Survey

DiBiase, D., King, B. F., Stroh, W., Baxter, R., & Sloan, J. L. (2016). *The nature of geographic information*. Retrieved October 31, 2021, from https://www.e-education.psu.edu/natureofgeoinfo/

Environmental Protection Agency (EPA). (2016). *Wetlands classification and types*. Retrieved November 1, 2021, from https://19january2017snapshot.epa.gov/wetlands/wetlands-classification-and-types_.html#marshes

Environmental Protection Agency (EPA). (2021a). *About Waters of the United States*. Retrieved October 31, 2021, from https://www.epa.gov/wotus/about-waters-united-states

Environmental Protection Agency (EPA). (2021b). *Vernal pools*. Retrieved October 31, 2021, from https://www.epa.gov/wetlands/vernal-pools

Esri. (n.d.-a). *Clip raster (data management)*. Retrieved October 31, 2021, from https://pro.arcgis.com/en/pro-app/latest/tool-reference/data-management/clip.htm

Esri. (n.d.-b). *Create polygon features*. Retrieved October 31, 2021, from https://pro.arcgis.com/en/pro-app/latest/help/editing/create-polygon-features.htm

Esri. (n.d.-c). *Fill (spatial analyst)*. Retrieved October 31, 2021, from https://pro.arcgis.com/en/pro-app/latest/tool-reference/spatial-analyst/fill.htm

Esri. (n.d.-d). *How inverse distance weighted interpolation works*. Retrieved October 31, 2021, from https://pro.arcgis.com/en/pro-app/latest/help/analysis/geostatistical-analyst/how-inverse-distance-weighted-interpolation-works.htm

Esri. (n.d.-e). *LAS dataset to raster (conversion)*. Retrieved October 31, 2021, from https://pro.arcgis.com/en/pro-app/latest/tool-reference/conversion/las-dataset-to-raster.htm

Esri. (n.d.-f). *Mosaic to new raster (data management)*. Retrieved October 31, 2021, from https://pro.arcgis.com/en/pro-app/latest/tool-reference/data-management/mosaic-to-new-raster.htm

Esri. (n.d.-g). *Project raster (data management)*. Retrieved October 31, 2021, from https://pro.arcgis.com/en/pro-app/latest/tool-reference/data-management/project-raster.htm

Esri. (n.d.-h). *Python migration from 10.x to ArcGIS Pro*. Retrieved October 31, 2021, from https://pro.arcgis.com/en/pro-app/latest/arcpy/get-started/python-migration-for-arcgis-pro.htm

Esri. (n.d.-i). *Resample (data management)*. Retrieved October 31, 2021, from https://pro.arcgis.com/en/pro-app/2.7/tool-reference/data-management/resample.htm

Esri. (2021a). *ArcGIS Pro* (Version 2.8). https://www.esri.com/en-us/arcgis/products/arcgis-pro/overview

Esri. (2021b). *ArcMap* (Version 10.8). https://www.esri.com/en-us/arcgis/products/arcgis-desktop/resources

Fisher, J. & Acreman, M. C. (2004). Wetland nutrient removal: a review of the evidence. *Hydrology and Earth System Sciences Discussions*, *8*(4), 673-685. https://hal.archives-ouvertes.fr/hal-00304953

GISGeography. (2021). *A complete guide to LiDAR: Light detection and ranging*. Retrieved October 31, 2021, from https://gisgeography.com/lidar-light-detection-and-ranging/

Huertos, M. L. (2020). Chapter 7 - The stage: Typologies of aquatic systems. In *Ecology and Management of Inland Waters: A Californian Perspective with Global Applications* (pp. 225–256). Elsevier. Retrieved October 31, 2021, from https://doi.org/10.1016/B978-0-12-814266-0.00020-9

Jensen, C. K., McGuire, K. J., McLaughlin, D. L., Scott, D. T. (2019). Quantifying spatiotemporal variation in headwater stream length using flow intermittency sensors. *Environmental Monitoring Assessment, 191*(226). https://doi.org/10.1007/s10661-019-7373-8

Jin, S., Homer, C., Yang, L., Danielson, P., Dewitz, J., Li, C., Zhu, Z., Xian, G., Howard, D. (2019). Overall methodology design for the United States National Land Cover Database 2016 products. *Remote Sensing*, *11*(24), 2971. https://doi.org/10.3390/rs11242971

Julian, J. (2018). *Vernal pools—Seasonal ponds for special amphibians*. The Spring Creek Watershed Atlas. Retrieved October 31, 2021, from https://www.springcreekwatershedatlas.org/post/2018/12/19/vernal-pools-seasonal-ponds-for-special-amphibians

Khan, A. (2020). *Understanding terrain features for landscaping*. JD Institute of Fashion. Retrieved October 31, 2021, from https://jdinstitute.co/understanding-terrain-features-for-landscaping/

Lathrop, R. G., Montesano, P., Tesauro, J., Zarate, B. (2005). Statewide mapping and assessment of vernal pools: A New Jersey case study. *Environmental Management*, *76*(3), 230-238. https://doi.org/10.1016/j.jenvman.2005.02.006

Leibowitz, S. G. & Brooks, R. T. (2008). Hydrology and landscape connectivity of vernal pools. In (A. J. K. Calhoun & P. G. deMaynadier, Eds.), *Science and Conservation of Vernal Pools in Northeastern North America* (pp. 31–53). CRC Press

Lindsay, J. B. (2016). Whitebox GAT: A case study in geomorphometric analysis. *Computers & Geosciences*, *95*(C), 75-84. doi:10.1016/j.cageo.2016.07.003

Lindsay, J.B. (2021). *WhiteboxTools user manual*. University of Guelph, Geomorphometry and Hydrogeomatics Research Group

Lindsay, J. B. & Creed, I. F. (2005). Sensitivity of digital landscapes to artifact depressions in remotely-sensed DEMs. *Photogrammetric Engineering & Remote Sensing*, *71*(9), 1029-1036. doi: 10.14358/PERS.71.9.1029

Lindsay J. B. & Creed I. F. (2006). Distinguishing between artefact and real depressions in digital elevation data. *Computers and Geosciences*, *32*(8), 1192-1204. doi: 10.1016/j.cageo.2005.11.002

Lindsay, J. B. & Dhun, K. (2015). Modelling surface drainage patterns in altered landscapes using LiDAR. *International Journal of Geographical Information Science*, *29*(3), 397-411. doi: 10.1080/13658816.2014.975715

MacFaden, S. W., Raney, P. A., O'Neil-Dunne, J. (2021). LiDAR-aided hydrogeologic modeling and object-based wetland mapping approach for Pennsylvania. *Applied Remote Sensing*, *15*(2). https://doi.org/10.1117/1.JRS.15.026503

Machtinger, E. T. (2007). (R. Marks, W. Hohman, B. LaPage, N. Barrett, L. Frederickson, & B. Weihrouch, Eds.) *Temporarily flooded wetlands*. Natural Resources Conservation Service

Marsh, B. (1999). *Paleoperiglacial landscapes of Central Pennsylvania* (Vol. 62). Lewisburg, Pennsylvania: Bucknell University

Microsoft. (2021a). *Excel* (Version 2110). https://www.microsoft.com/en-us/microsoft-365/excel

Microsoft. (2021b). *PowerPoint* (Version 2110). https://www.microsoft.com/en-us/microsoft-365/powerpoint

National Oceanic and Atmospheric Administration (NOAA). (2021). *What is LiDAR*. NOAA National Ocean Service. Retrieved October 31, 2021, from https://oceanservice.noaa.gov/facts/lidar.html

Parry, S. (2011). Chapter 15- The application of geomorphological mapping in the assessment of landslide hazard in Hong Kong. In *Developments in Earth Surface Processes* (pp. 413-441). Elsevier. Retrieved October 31, 2021, from https://doi.org/10.1016/B978-0-444-53446-0.00015-X

Pennsylvania Department of Conservation and Natural Resources (PADCNR). (2001). *Bedrock geology of Pennsylvania*. Pennsylvania Spatial Data Access. https://www.pasda.psu.edu/uci/DataSummary.aspx?dataset=480

Pennsylvania Department of Conservation and Natural Resources (PADCNR). (2006-2008). *PAMAP Program- 3.2 ft Digital Elevation Model*. Pennsylvania Spatial Data Access. https://www.pasda.psu.edu/uci/DataSummary.aspx?dataset=1247

Pennsylvania Department of Transportation (PennDOT). (2015). *Wetland Resources Handbook* (Pub. 325)

Pennsylvania Natural Heritage Program (PNHP). (2019). *Vernal pools*. Retrieved October 31, 2021, from http://www.naturalheritage.state.pa.us/VernalPools.aspx

Pennsylvania Spatial Data Access (PASDA). (2021). *Pennsylvania Imagery Navigator*. Retrieved October 31, 2021 from https://maps.psiee.psu.edu/ImageryNavigator/

Planchon, O. & Darboux, F. (2002). A fast, simple and versatile algorithm to fill the depressions of digital elevation models. *Catena*, *46*(2-3), 159–176. doi: https://doi.org/10.1016/S0341-8162(01)00164-3

Senseny, P. E. & Pfeifle, T. W. (1984). *Fracture toughness of sandstones and shales*. The 25th U.S. Symposium on Rock Mechanics (USRMS), Evanston, Illinois

Smith, H. (2020). *Projection on the fly and geographic transformations*. Retrieved October 31, 2021, from https://www.esri.com/arcgis-blog/products/arcgis-pro/mapping/projection-on-the-fly-and-geographic-transformations/

Stevens, C. M. (2011). *Hydrologic indicators*. US Army Corps of Engineers, Coastal Branch

Stolt, M. H. & Baker, J.C. (1995). Evaluation of National Wetland Inventory maps to inventory wetlands in the Southern Blue Ridge of Virginia. *Wetlands*, 15(4), 346-353

Tiner, R. W. (2003). Geographically isolated wetlands of the United States. *Wetlands*, *23*(3), 494–516. https://doi.org/https://doi.org/10.1672/0277-5212(2003)023[0494:GIWOTU]2.0.CO;2

United States Department of Agriculture (USDA) & Natural Resources Conservation Service (NRCS). (2006). *Land resource regions and major land resource areas of the United States, the Caribbean, and the Pacific Basin*. USDA Handbook 296

United States Fish and Wildlife Service (USFWS). (1983). *Wetlands Mapper*. National Wetlands Inventory. https://www.fws.gov/wetlands/data/Mapper.html

United States Fish and Wildlife Service (USFWS). (2020). *NWI program overview*. National Wetlands Inventory. Retrieved October 31, 2021, from https://www.fws.gov/wetlands/nwi/overview.html

United States Geological Survey (USGS). (2017). *USGS QL2 LiDAR for Mifflin County, PA 2017*. Pennsylvania Spatial Data Access. https://www.pasda.psu.edu/uci/DataSummary.aspx?dataset=1807

Wang, L. & Liu, H. (2006). An efficient method for identifying and filling surface depressions in digital elevation models for hydrologic analysis and modelling. *International Journal of Geographical Information Science*, *20*(2), 193-213. doi: 10.1080/13658810500433453

Western Pennsylvania Conservancy (WPC). (2018). *Vernal pools*. Retrieved October 31, 2021, from https://waterlandlife.org/wildlife-pnhp/special-places-2/vernal-pools/

Wu, Q., Lane, C., Liu, H. (2014). An effective method for detecting potential woodland vernal pools using high-resolution LiDAR data and aerial imagery. *Remote Sensing*, *6*(11), 11444–11467. doi:10.3390/rs61111444

Wu, Q., Liu, H., Wang, S., Yu, B., Beck, R., Hinkel, K. (2015). A localized contour tree method for deriving geometric and topological properties of complex surface depressions based on high-resolution topographical data. *International Journal of Geographical Information Science*, *29*(12), 2041-2060. doi: 10.1080/13658816.2015.1038719

Wu, Q. & Lane, C. R. (2017). Delineating wetland catchments and modeling hydrologic connectivity using lidar data and aerial imagery, *Hydrology and Earth System Sciences*, *21*(7), 3579–3595. https://doi.org/10.5194/hess-21-3579-2017

YellowScan. (2020). *How does LiDAR work?*. Retrieved October 31, 2021, from https://www.yellowscan-lidar.com/knowledge/how-lidar-works/

ACADEMIC VITA

Ritvik Prabhu

ritvik.prabhu36@gmail.com

EDUCATION

THE PENNSYLVANIA STATE UNIVERSITY
State College, PA
Environmental Resource Management
(Water Science Option)
Minors: Biological Eng., Environmental Eng.
(Expected graduation Dec 2021)

Awards & Honors
- Schreyer Honors College
- Dean's List, 6 Semesters

ADDITIONAL SKILLS

Attention to Detail

Quick Learner and Adaptable

ArcGIS Pro Experience

Basic Wetland and Stream Delineation

CERTIFICATIONS

PA NC Class C Drivers License

REFERENCES

References available upon request

EXPERIENCE

PENN STATE OUTING CLUB
State College, PA / Sep 2018 - Present
- Currently working to set up safer University-approved backpacking system using the Common Adventure Model
- **Webmaster**, *Dec 2020 – Present*
- **Vice President**, *Dec 2019 - Dec 2020*
  Oversaw all officer positions
- **Social Chair**, *Dec 2018 - Dec 2019*

HONORS THESIS RESEARCH
State College, PA / Dec 2020 - Present
- Determining best practices for vernal pool morphology modeling in headwater regions

PENN STATE IT HELP DESK CONSULTANT
State College, PA / Sep 2019 - Present
- Worked call center for IT and General questions
- Trained employees and updated knowledge documentation

PHI KAPPA TAU FRATERNITY
State College, PA / Mar 2019 – August 2021
- Philanthropy Chair, *Dec 2019 – Dec 2020*

APOLLO
State College, PA / Sep 2018 - Present
- Org. dedicated to raising money for philanthropy THON

PROGRAMMING INTERN
Yoink LLC, Wayne, PA / Aug 2017 - Aug 2018
- Learned coding skills (primarily in Clojure language) while living remotely in Mexico City for Cloud-Native company

CONSERVATION VOLUNTEER
Various Locations / March 2018 - Apr 2018
- Assisted with maintenance, conservation practices, wildlife monitoring, and rehabilitation
- Kariega Game Reserve, Eastern Cape, South Africa, *3 weeks*
- Hanson Bay Wildlife Sanctuary, Southern Australia, *2 weeks*
- Cairns Turtle Rehabilitation, Queensland, Australia, *1 week*

BOY SCOUTS OF AMERICA
Troop 284, Radnor, PA / Sep 2012 - May 2017
- Eagle Scout, *Jan 2017*

SUMMER INTERN
Clean Air Council, Philadelphia, PA / Jun 2016 - Aug 2016
- Had duties ranging from informational campaigns to donor analysis to correspondence with other NGOs